Masaryk University in Brno
Faculty of Science
Department of Organic Chemistry

Diploma Thesis

The Application of Microwave-Assisted Photochemistry

Pavel Müller

2004

Acknowledgements

I would like to thank my mentor, Assist. Prof. RNDr. Petr Klán, Ph.D. for the opportunity to work in the field of microwave photochemistry under his supervision.

I acknowledge the helpfulness of my colleagues and Organic Chemistry Department employees, namely Jaromír Literák, Dominik Heger, Radovan Růžička, Tomáš Pospíšil, and Assist. Prof. RNDr. Pavel Janderka, CSc.

I also appreciate the aid of Socrates-Erasmus student exchange program and help of my colleagues from University of Paris-South XI, particularly that of Prof. André Loupy, Didier Gori and Alain Petit.

I further thank to Dr. Ing. Vladimír Církva for the manufacturing of numerous electrodeless discharge lamps.

I also appreciate the help of RNDr. Zbyněk Boháček from the Czech Geological Survey, who purified and supplied the hydrocarbons necessary for my experiments.

Last but certainly not least, I would like to thank my parents and my whole family for the support they have given me during my studies.

Contents

Introduction

This thesis strives to report on our research into applications of simultaneous ultraviolet and microwave irradiation to organic samples. The attention is aimed namely to the utilization of the electrodeless discharge lamps (EDLs), powerful photochemical tools emitting light in the UV/VIS spectral region upon placement in the microwave field. Spectra of diverse EDLs (under various conditions) are presented, followed by a discussion of the advantages and limitations of their use.

The second part of the thesis informs on our study of the temperature effects on several photochemical reactions such as Norrish type II reactions, Paternò-Büchi reactions, and photochemically induced S_NAr.

Chapter 1

Microwave Chemistry

Microwaves - people use them every day, cutting-edge technologies depend on them but they are as old as the universe. They are the magic behind radar, satellites, and cell phones. They make images of other planets possible, while helping people monitor the health of the Earth.

In 1986, Richard N. Gedye published a pioneering work on microwave-assisted organic synthesis [1]. Since then, the number of published papers dealing with microwave chemistry has been growing year by year.

Use of microwave heating has become popular among synthetic chemists all over the world mainly because it can reduce the reaction times, improve yields and sometimes even enhance the product purity.

1.1. Microwave Radiation, Microwave Spectroscopy

Microwave radiation is an electromagnetic radiation of frequencies ranging from 1 to 100 GHz (corresponding to wavelengths from 3 mm to 30 cm, Fig. 1.1). Domestic microwave ovens usually operate at 2.45 GHz.

Microwave spectroscopy is a method, which is not very often used by organic chemists but it can give useful information - information about the size and shape of molecules. Rotational levels are dependent on the moment of inertia, which can be

calculated from the positions of the peaks in microwave spectra. From these, bond distances, angles dipole moments and rotational barriers may be calculated [2].

Microwave spectroscopy is applicable to gases at low pressures and only to compounds with dipole moments. Only purely rotational transitions can be found in the microwave spectral region. The peaks do not overlap and are not characteristic of groups within a molecule [2].

Fig. 1.1. Electromagnetic spectrum – frequencies and wavelengths.

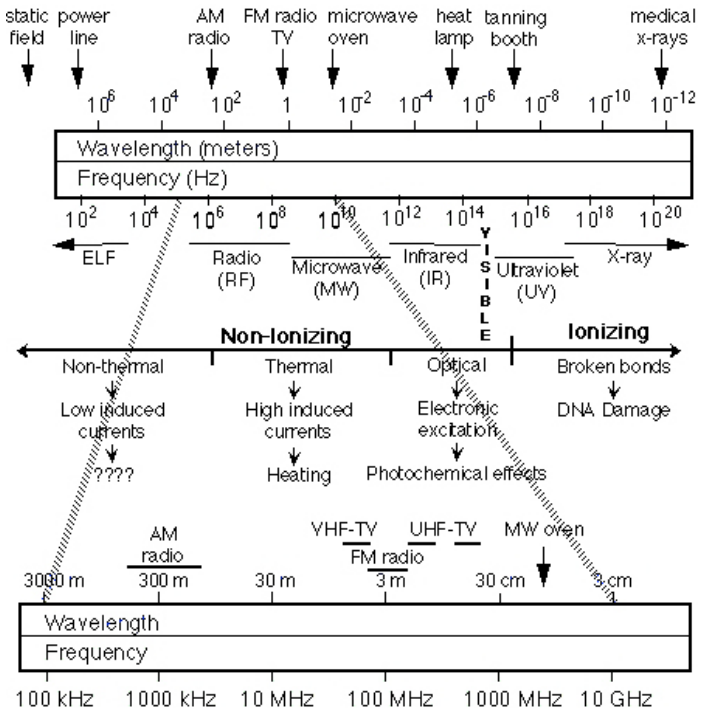

1.2. Microwave Heating

Microwave heating results from conduction losses and dielectric polarization. Conduction losses are caused by migration of charged particles in the electric field. Dielectric heating is a consequence of dipole-dipole interactions between polar

molecules and the electric field. Permanent and induced dipoles in the dielectric material try to align with an alternating electric field, which results in their rotation and intermolecular friction and thereby in heat.

The overall polarization consists of four main components: electric, atomic, dipolar and interfacial polarization. Electric polarization results from realignment of electrons around nuclei. Atomic polarization is a consequence of the relative displacement of nuclei due to changed electron distribution in the molecule. Dipolar polarization arises from the orientation of permanent dipoles in the electric field. Interfacial polarization occurs in case that charges appear at the interfaces.

Electric and atomic polarizations and depolarizations are much faster than electric field alternations. These two components of polarization therefore do not contribute to the microwave dielectric heating.

When the applied oscillating electric field changes direction slowly, the permanent dipole moment has time to reorientate – the whole molecule rotates into a new direction – and follow the field. However, when the frequency of the field is higher, the molecule cannot change direction fast enough to follow the change in direction of the applied field. The shift behind the electric field oscillation indicates that the matter absorbs energy from the field and heats up [3].

The ability of the medium to be polarized by electric field can be described by a dimensionless parameter – the relative permittivity, ε_r, which is also called the dielectric constant. The relative permittivity can also have a very significant effect on the strength of the interaction between ions in solution. For instance, water has a relative permittivity of 78 at 25 °C, so the interionic Coulombic interaction energy is reduced by nearly two orders of magnitude from its vacuum value.

The relative permittivity of a substance is a measure of its polarity and/or polarizability. The value of relative permittivity may vary with temperature.

For example, water permittivity decreases significantly with the increasing temperature and its value at about 180 °C is close to that of some less polar solvents (e.g. acetonitrile) at room temperature [4]. Apart from other things, this phenomenon is of interest in the context of green chemistry because even non-polar organic compounds, which are water-insoluble at room temperature, may dissolve in water when the temperature is higher. Water may thus substitute for environment-unfriendly organic solvents in many cases.

1.3. Microwave Effects

1.3.1. Superheating Effect

The solvents efficiently absorbing microwave energy very often start to boil at higher temperatures than under conventional heating conditions. This phenomenon, called the superheating effect, has been attributed to a slower nucleation under microwave heating and can only be observed in the absence of nucleation regulator (boiling chips, stirring).

Table 1.1. Atmospheric pressure boiling points of some polar solvents for both conventional and MW heating [5,6].

Solvent (type)	Boiling point (°C)	MW heating B.p. (°C)	B.p. increase (°C)
Water (III)	100	105	5
Methanol (II)	65	84	19
Propan-2-ol (I)	117	138	21
Butan-1-ol (II)	118	132	14
Acetone (II)	56	89	33
Ethyl acetate (I)	77	102	25
Dichloromethane (I)	40	55	15
Acetonitrile (II)	82	120	38

Common solvents can generally be divided into three classes, according to their behavior during microwave heating [6]. The first-class solvent (solvent type I, e.g. ethanol, Fig. 1.2) is heated to the boiling point but the temperature keeps on rising up to a certain point (maximum), at which solvent bumps and starts to reflux vigorously; the temperature drops to a plateau and remains there for some time. After this time, the temperature decreases slowly to the solvent boiling point. The second-class solvent (solvent type II, e.g. methanol) is heated to a temperature higher than its boiling point but it does not bump. The third-class solvent (solvent type III, e.g. water) can be heated up to a temperature, which is only very slightly higher than the boiling point.

Fig 1.2. Superheating of polar solvents (type I, EtOH, [6]).

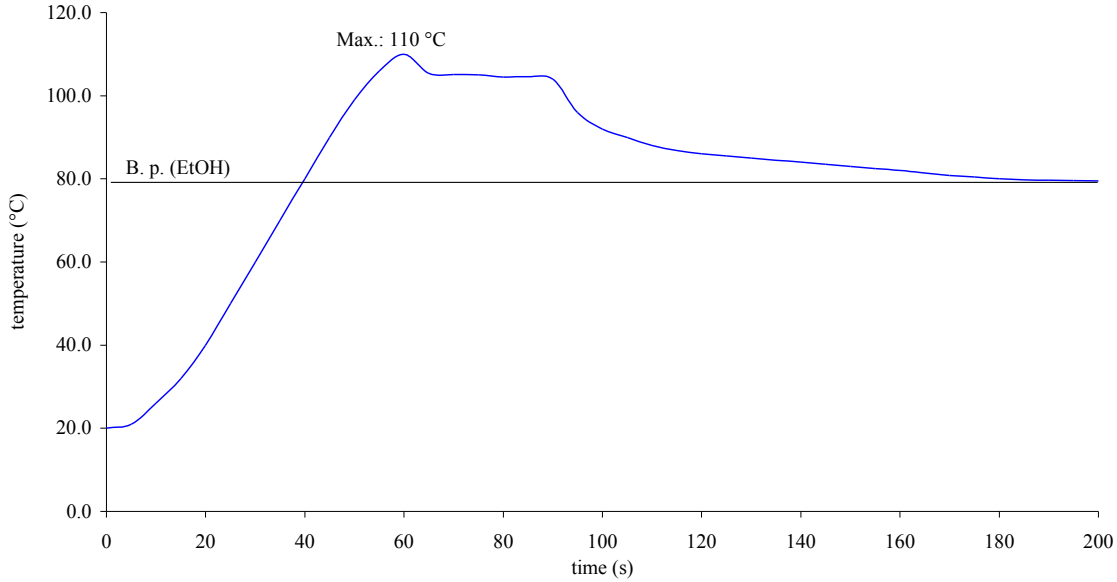

1.3.2. Microwave Stabilization of Polar Species, Specific MW Effect

In the past, a couple of authors published a number of articles comparing the reactions conducted in the microwave field with the reactions carried out under normal (thermal) conditions. The sometimes unequal results made them suggest there might be a specific non-thermal microwave effect [5,7]. They expected a stabilization of polar

species by microwave field. If such a stabilization of the reaction transition state occurred and was more pronounced than that of the ground state, the activation energy would decrease and the reactivity would be enhanced. The reaction pathways with less-polar transition states would thus be suppressed in favor of those with more-polar transition states.

Lately, a questionable reproducibility of the previous experiments and possible explanations of most of the unequal results within the scope of thermal effects made most of the microwave chemists abandon the contemplations about the non-thermal specific microwave effects.

1.4. Magnetic Field Effects

All chemical reactions are spin-selective. Only spin-allowed reaction channels are open, whereas the others, even if they are energetically permissible, are strictly closed for the reactions. The only interactions that are able to disturb the spin of reagents and transform the non-reactive (spin-forbidden) reagent states into reactive (spin-allowed) ones (and vice versa) are the magnetic interactions [8].

Fig. 1.3. The scheme of spin orientations of two unpaired electrons in triplet states T_{+1}, T_0, T_{-1}, and in singlet state S [8].

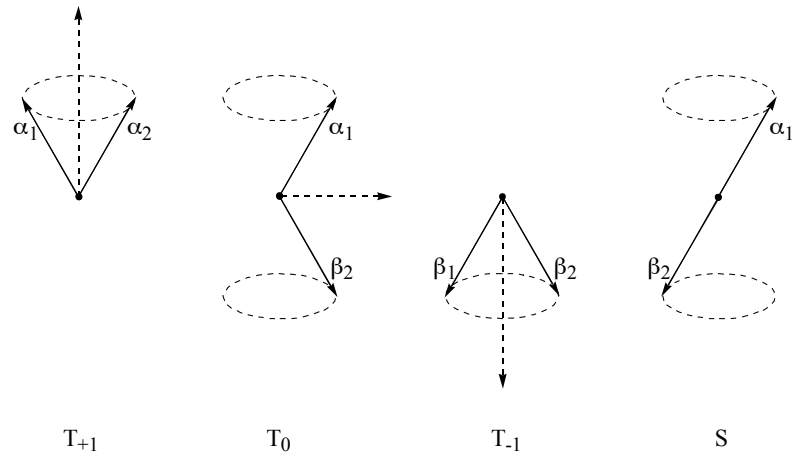

The organization of electron spins determines the spin state. The total spin of two radicals (e.g. in the radical pair) can be equal to ±1 (the spins of individual radical partners are summed up) or to 0 (the spins are compensated). Accordingly, the radical pair can be in triplet T or singlet S spin states (Fig. 1.3). The interconversion between these two spin states is called intersystem crossing (ISC).

1.4.1. Singlet-Triplet Interconversion

It was already mentioned that singlet and triplet states are interconvertible by an external magnetic field. The processes leading to this interconversion are called spin rephasing or spin flip (Fig. 1.4).

Fig. 1.4. Schematic representation of spin rephasing and spin flip in a magnetic field H [9].

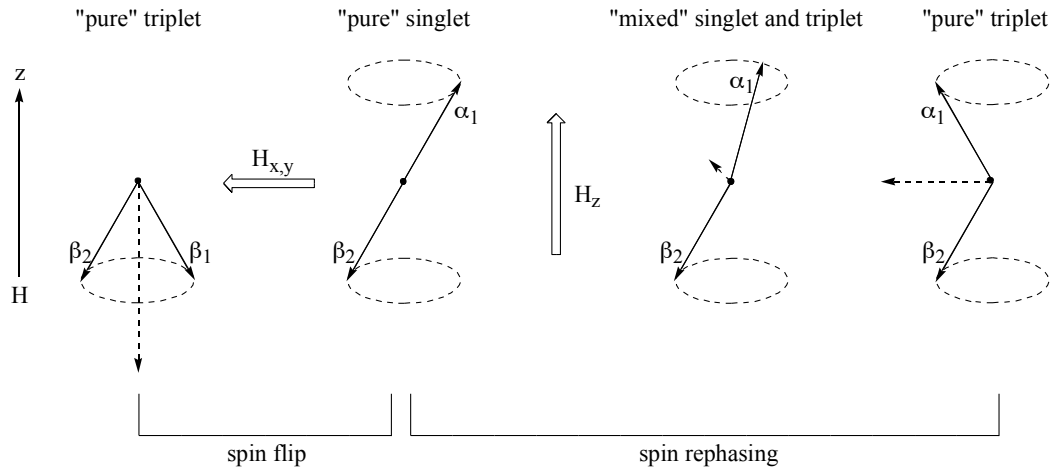

1.4.2. ISC Induced by Oscillating Magnetic Field

In zero and very low magnetic fields, the singlet and triplet states of the radical pair are almost degenerated and the spin dynamics involves all four states (T_{-1}, T_0, T_{+1} and S) into the spin conversion. Nevertheless, the applied external magnetic field

increases the energetic difference (ΔE) between the T_0 and $T_{\pm1}$ states, which thus cease to be degenerated (the stronger the applied magnetic field, the higher the ΔE value). The spin multiplicity interconversions S – $T_{\pm1}$ are then no longer allowed and the T – $T_{\pm1}$ transitions become very slow (due to the energy difference) [8].

The oscillating magnetic field can to a large extent change the dynamic behavior of the radical pair. In high magnetic fields, e.g. in an EPR spectrometer, the T_0 – S interconversion empties the population of the T_0 state. The resonant microwave radiation (oscillating magnetic field) stimulates the $T_{\pm1}$ – T_0 transitions and thus increases the yield of the ISC [10].

Hore and coworkers [11–13] recently described the effects of time-dependent magnetic field (created by electromagnetic waves) in the absence of a strong magnetic field. They observed that the radiofrequency radiation that matches energy level splitting arising from hyperfine interaction can decrease the fluorescence intensity of singlet radical ion pair. They refer to this phenomenon as the oscillating magnetic field effect, OMFE.

According to the OMFE model presented by Timmel and Hore, a weak oscillating magnetic field (the magnetic interactions are much smaller than the thermal energy of the molecule) has no impact on equilibrium constants or activation energies, however, it can have an immense kinetic control over the reaction of the radicals (the oscillating magnetic field influences the state mixing of the radical pair – $k_{T\rightarrow S}$ and $k_{S\rightarrow T}$) [14].

There is still an open question if electromagnetic fields influence animal and human physiology. For instance, it has been suggested that radiofrequency fields may disorient birds [15]. There are, however, no detailed experimental studies of the OMFE in the microwave region yet.

1.5. Microwave Photochemistry

There have been attempts to affect photochemical reactions by other sources of non-classical activation, such as ultrasound [16–18] or magnetic field [19,20]. Photochemistry in the microwave field [21] presents a combined chemical activation by two distinctive kinds of electromagnetic radiation. Energy of microwave radiation (E = 0.4–40 J.mol^{-1} at ν = 1–100 GHz) is considerably lower than that of UV-VIS radiation (E = 600–170 kJ.mol^{-1} at λ = 200–700 nm), thus insufficient to disrupt bonds of common organic molecules.

It has already been explained in Subchapter 1.2 that microwave heating is not identical to classical external heating, at least at the molecular level [22–25]. Molecules with a permanent (or induced) dipole respond to an electromagnetic field by rotating, which results in friction with neighboring molecules, thus in heat.

There are some additional (secondary) effects of microwaves, including ionic conduction (ionic migration in the presence of electric field) or spin alignment. Therefore, MW effects on photochemical reactions are expected to be diverse.

Simultaneous applications of UV and MW irradiation have found a widespread use in industry. For instance, microwave photochemistry proved to be quite advantageous for removal of a toxic material or pathogens from wastewater [21]. During a process called photochemical oxidation, a strong oxidizing reagent (O_3 or H_2O_2) is added to water in an UV-ionizing reactor resulting in generation of highly reactive hydroxyl radicals (OH·), which react with numerous toxic compounds and efficiently kill most microorganisms.

Chapter 2

Electrodeless Discharge Lamp

The objective of photochemistry in the microwave field is frequently, but not irreplaceably, connected to the electrodeless discharge lamp (EDL), which generates UV radiation when placed into the MW field.

2.1. Principle of EDL Operation

The electrodeless discharge lamp is a glass tube filled with an excitable substance and sealed under a reduced pressure or a noble gas. A high frequency electromagnetic field (radio frequency or MW, 300–3000 MHz) can trigger gas discharge causing the emission of electromagnetic radiation (Fig. 2.1). This phenomenon has been studied for many years and was already well understood in the 1960s [26].

Electrodeless discharge lamp is usually characterized by higher emission intensity than the hollow cathode lamps, a lower contamination due to the absence of the electrodes, and a longer lifetime [21].

EDLs operate due to free electrons in the fill that are accelerated by the energy of the MW field. They collide with the gas atoms and ionize them to release more electrons (the “avalanche” effect).

The energetic electrons collide with heavy-atom particles present in the plasma, thus exciting them from the ground state to higher energy levels. The excitation energy

is then released as an electromagnetic radiation with the spectral characteristics depending on the composition of the fill.

Fig. 2.1. Diagram of EDL operation.

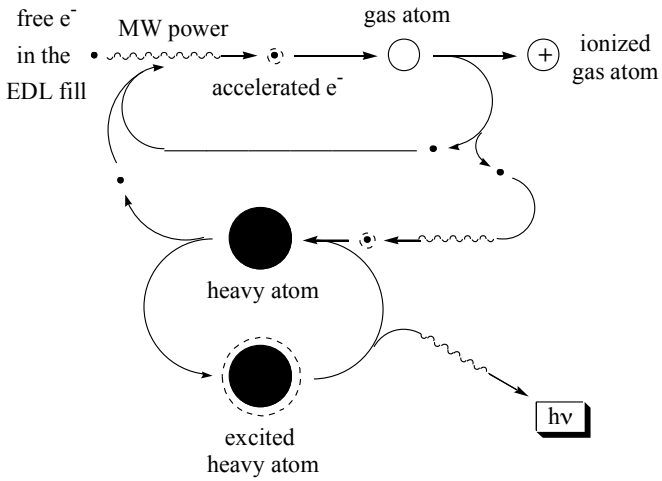

2.2. Parameters Affecting EDL Performance

There are a number of operating parameters [21], which have been recognized as influencing the electrodeless discharge lamp performance, such as temperature, nature and pressure of the fill gas, choice of the fill material, dimensions of the lamp envelope, the nature and characteristics of the MW energy coupling device, and the frequency and intensity of the MW energy.

The effect of temperature on EDL is closely associated with the fill gas pressure. At room temperature ($T \approx 300$ K) the gas mixture in the lamp has a pressure of approximately 2.6 kPa (0.026 atm), while in an operation mode the temperature of the plasma is most likely between 700 and 1400 K, and the pressure about 1MPa (10 atm) [27].

The plasma includes strong non-equilibrium states due to high-energy particles. The plasma pressure influences the characteristics of the radiation; it affects the mean free path of the particles and their collisional cross-sections. Pressure thus affects the number of collisions per unit of time.

Lower-state atoms, which are outside the plasma but still within the lamp volume, have a lower temperature than the emitting atoms within the plasma. Therefore, their absorption line profile is narrower than the emission line profile from the plasma [27].

The spatial distribution and relative concentrations of emitting and absorbing atoms critically depend on the partial pressure of the element within the discharge volume: the higher the partial pressure of the element, the more lower-state atoms exist outside the emitting plasma. Therefore, more self-absorbed and self-reversed atomic lines result from the simultaneous presence of emitting atoms and lower-state atoms.

The effect of temperature on radiance from the electrodeless discharge lamps was already investigated [27–29]. It was found that the optimum operating temperature for the mercury fill is 42 °C (for 253.7 nm line, 6^1S_0–6^3P_1). The output is reduced when the temperature is beyond optimum. Operation at high power or high temperatures can increase the intensity but, at the same time, reduce the lifetime and also lead to a broadening of the atomic line profile due to self-absorption and self–reversal effects. The temperature dependence of emission intensities from mercury atoms at steady state for lines 365, 405, 436, 546 and 579 nm was also investigated [30].

The increase of the line emission intensities above 37 °C is explained by a decrease of the activation energy of mercury atoms or ions and by reduction of the number of interactions amongst mercury atoms in plasma.

The influence of the lamp cooling by air stream, that can cause lamp emission instability, was also examined [31]. If the vapor pressure in EDL is too high, the discharge may be limited or even extinguished completely [32].

2.3. Photochemical Reactor Containing EDL

The example of EDL application to organic photochemistry was shown by Klán and Hájek, who reported on an original microwave photochemical reactor. Such a reactor consisted of a flask containing EDL directly in the reaction mixture (Fig. 2.2) [33–35]. Such an arrangement was proposed for the first time by Den Besten and Tracy [36], and later applied by Církva and Hájek [37] in experiments using a modified microwave oven.

Fig. 2.2. Photochemistry in the MW field (adapted according to Klán, Hájek and Církva [35]).

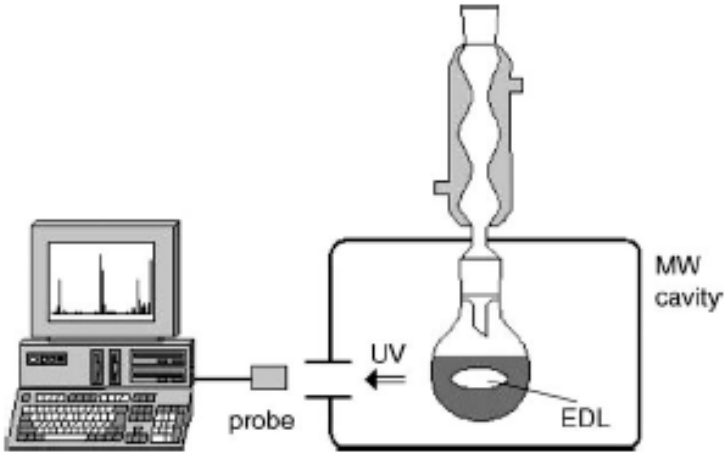

The modified microwave oven contained an external reflux condenser and a cooling glass spiral for removing redundant microwave energy, thus preventing the magnetron from destruction by overheating [35,38].

Photochemical applications of a microwave-powered light source in photochemistry were recently described in several articles [39–44]. Knowledge of spectral characteristics of EDL is clearly essential for planning the photochemical experiment. The right choice of a filling and envelope material, glass, and even temperature can dramatically modify the emission spectrum.

The influence of the EDL properties, the MW output power, and the reaction conditions on the EDL spectral characteristics will be discussed in more detail in Chapter 5.

Chapter 3

Temperature-Sensitive Photoreactions

Photochemical reactions in general are not very sensitive to temperature. The reacting species absorbs photon and is already high enough in energy to undergo a reaction. However, additional heating (no matter if conventional or microwave) may affect the reaction conversion, reaction selectivity, or even the ratio of the arising products.

3.1. Norrish Type II Reaction

Ketones with H-atom on γ-carbon can react upon irradiation according to a well-known Norrish Type II reaction, which is a reaction similar to McLafferty rearrangement known from the mass spectroscopy [45]. The emerging 1,4-biradical can cleave, cyclize (so-called Yang cyclization), or disproportionate back to the starting ketone (Scheme 3.1).

Scheme 3.1.

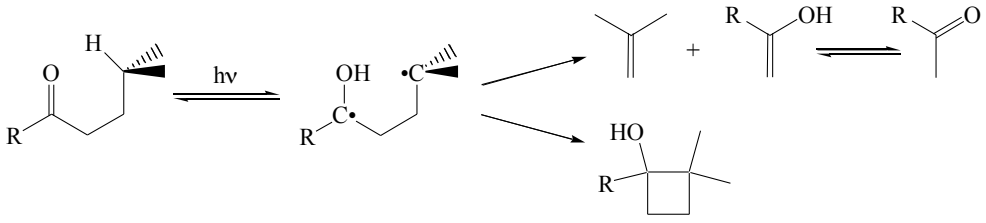

Wagner and Hammond suggested that it is the disproportionation of the 1,4-biradical what causes lower quantum yields of some Norrish type II reactions [46].

The evidence that 1,4-biradical really occurs on the reaction pathway was later given by Wagner [47] who observed photoracemization of ketones asymmetrically substituted in γ-position (Scheme 3.2). The photoracemization can take place due to the fact that the lifetime of 1,4-biradical is long enough for a rotation around the C_β-C_γ bond to occur.

Scheme 3.2.

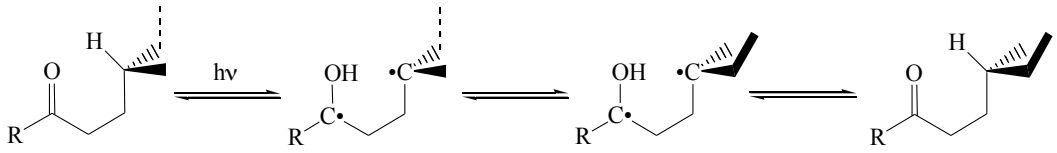

3.1.1. Triplet vs. Singlet Reaction Pathway

The hydrogen abstraction can occur both from a singlet $^1(n,\pi^*)$ and a triplet $^3(n,\pi^*)$ state. The quantum yields of triplet state reactions are generally higher than those of singlet state reactions. The hydrogen abstraction from the (π,π^*) excited state is virtually forbidden, regardless of its multiplicity [48].

The cyclization of aliphatic ketones occurs mostly from the $^3(n,\pi^*)$ state, which was demonstrated by a significant decrease in cyclization to fragmentation ratio when a triplet quencher was added.

Whereas both singlet and triplet states of aliphatic ketones undergo Norrish type II reaction, the aryl alkyl ketones (e.g. valerophenone and its derivatives) react mostly from $^3(n,\pi^*)$ state. The intersystem crossing (ISC) yields for such ketones are relatively high and the hydrogen abstraction therefore comes about predominantly from the triplet state.

3.1.2. Reactivity of Aryl Alkyl Ketones

The reactivity of aryl alkyl ketones changes significantly when a substituent is introduced in the *p*-position of the aromatic system. The electron donating substituents lower the energy of $^3(\pi,\pi^*)$. $^3(n,\pi^*)$ thus ceases to be the lowest triplet state and both rate constants and quantum yields decrease [49]. Table 3.1 shows rate constants of Norrish type II photoreaction for some *p*-substituted valerophenones including the population of their $^3(n,\pi^*)$ states.

Table 3.1. [49]

p-substituent	CF_3	H	$COOCH_3$	Alkyl	OCH_3
Hammet σ constant	0.54	0	0.45	-0.17	-0.27
rate constant [10^7 s^{-1}]	28	13	12	1.8	0.06
^{3}(n,π*) population [%]	99	99	40	18	1

The substituents in both γ- and δ-positions on the alkyl chain can also affect the rate constants of Norrish type II reactions. The rate constants increase with a decreasing C_γ-H bond strength. Electron withdrawing substituents in γ-position therefore decrease the reactivity, whereas electron-donating substituents enhance the hydrogen abstraction. Table 3.2 demonstrates the influence of substituents in γ-position on rate constants for several aryl alkyl ketones [49].

Table 3.2. [49]

γ-substituent	NR_2	phenyl	alkyl	H	CN
rate constant [10^7 s^{-1}]	80	40	14-20	0.7	0.4

In case of bulky substituents, geometric and conformational effects may come into play as well. The substituents in δ-position may influence the hydrogen abstraction through the inductive effect.

3.1.3. Fragmentation to Cyclization Ratio

The fragmentation to cyclization (F/C) ratio depends on a number of factors. Besides solvent properties (such as polarity, viscosity, etc.), pH and the wavelength of the used radiation, the ratio of arising photoproducts proved to be dependent also on the actual temperature of the reaction mixture [50]. The dependence of F/C ratio on temperature will be discussed in more detail in Chapter 5.

3.2. Photochemical S_NAr

While electrophilic substitution is the most common reaction on aromatic rings in the ground electronic state, nucleophilic substitution is typical for excited species [51]. The selectivity of photochemical S_NAr on several compounds appeared to be temperature-sensitive.

As reported by Klán and coworkers [40], photochemical S_NAr on *p*-nitroanisole by the OH^- anion in the environment of aliphatic alcohols yields two major products: *p*-methoxyphenol and *p*-nitrophenol (Scheme 3.3), the ratio of which depends markedly on the temperature. While *p*-methoxyphenol formation prevailed at lower temperatures (below 60 °C), *p*-nitrophenol turned out to be the major photoproduct at higher temperatures (80 °C and more).

Scheme 3.3.

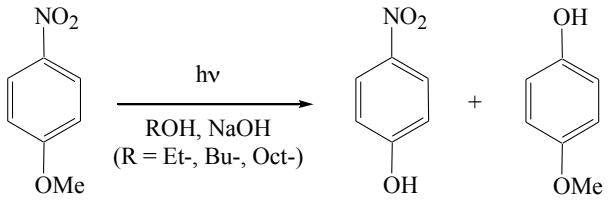

3.3. Paternò-Büchi Reaction

Carbonyl compounds in their *(n,π*)* excited states (both S_1 and T_1) undergo intermolecular photocycloadditions with ethylenes to form oxetane rings (Scheme 3.4). These reactions, known as Paternò-Büchi reactions, are rarely concerted, which is due to an insufficient orbital overlap of the cyclic transition state [48].

Scheme 3.4.

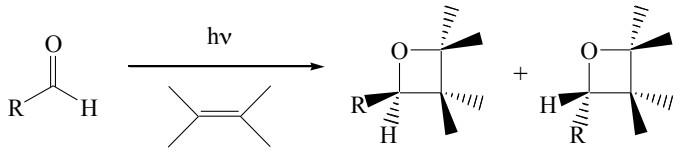

3.3.1. Perpendicular vs. Parallel Approach

There are two possible pathways leading to the products of the Paternò-Büchi reaction. The first pathway starts with an electrophilic attack launched by a reaction of *n*-orbital (SOMO) with π electrons of ethylene (HOMO). The second pathway starts with a nucleophilic attack launched by a reaction of a carbonyl π^* orbital (SOMO) with an empty π^* orbital (LUMO) of ethylene. The former one is referred to as a *perpendicular approach*, the latter as a *parallel approach* (Scheme 3.5).

Scheme 3.5.

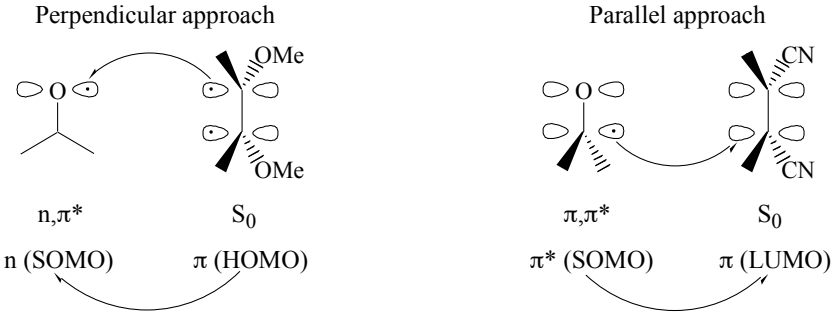

The perpendicular approach is typical for electron-rich ethylenes (such as enolethers, alkenes, dienes, etc.), i.e. for ethylenes with values of ionization potential lower than 9 eV. The parallel approach, on the other hand, is characteristic of electron-deficient ethylenes (halogenethylenes, cyanoethylenes, etc.). The lower is the ionization potential of electron-donating ethylene, the faster the reaction proceeds. Conversely, the rate constant of a reaction of electron-accepting ethylenes increases with the growing ionization potential [48].

3.3.2. Carbonyl Multiplicity

The multiplicity of the reacting excited state depends on the ketone structure. In the case of arylketones, the intersystem crossing from S_1 is very fast ($> 10^{10}$ s^{-1}); oxetanes are therefore formed exclusively from the T_1 excited state. Dialkylketones (such as acetone), on the other hand, have a long-lived S_1 state. The reaction can thus occur from both S_1 and T_1 excited states [9].

The aforementioned excited states yield quantitatively different products. Whereas the S_1 states mark out by a substantial stereoselectivity, the T_1 states usually give more stereoproducts.

Photocycloadditions are often accompanied by other events such as hydrogen abstraction, electron transfer and/or energy transfer.

3.3.3. Spin-Directed Stereoselectivity, Temperature and Viscosity Effects

Griesbeck et al. [52] investigated the impacts of various factors on the stereoselectivity of the Paternò-Büchi reactions using 2,3-dihydrofurane and various aldehydes as starting compounds (Scheme 3.6).

Scheme 3.6.

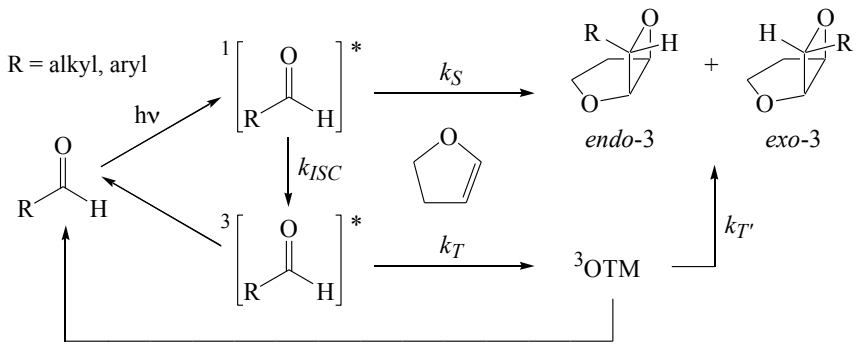

They analyzed not only the effects of temperature but also those of solvent viscosity and concentration of reacting compounds. The goal was to assess the influence of the intersystem crossing process from the 2-oxatetramethylene triplet 1,4-biradical (^{3}OTM, Scheme 3.7) to the closed-shell product on the final reaction stereoselectivity.

Scheme 3.7.

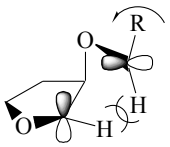

^{3}OTM

The increasing solvent viscosity proved to enhance the formation of *endo*-products. This effect was attributed to the preference of the ISC (S → T) to the reaction of the singlet excited species with 2,3-dihydrofuran due to the reduction in a diffusion rate limit.

Scheme 3.7 illustrates a steric hindrance of the hydrogen atom in position 2 of the furan ring, which predetermines a preferred transformation of the ^{3}OTM into *endo*-products. When the reaction of a singlet carbonyl takes place, a moderate *exo*- selectivity can be observed (up to 65 %).

Each pair of the tested carbonyl and alkene components exhibited a characteristic substrate concentration at which point a 1:1 ratio of singlet and triplet reactivity (i.e. spin selectivity) could be detected. The concentration/stereoselectivity correlations reflected the different kinetic contributions to the complex reaction scenario (Scheme 3.6).

Because the lifetime of the excited singlet state of aliphatic aldehydes is of the order of 1 ns [53], the reaction probability from the singlet channel is restricted by molecular diffusion. Under such conditions, the photophysical deactivation processes compete with the photochemical channels. Therefore, the probability of reaction from the singlet channel in dilute solutions decreases, whereas the probability of triplet state population increases. On the other hand, when the concentrations of the reacting species are too high, other processes such as bimolecular quenching of the singlet and triplet aldehyde by the ground-state aldehyde have to be taken into consideration.

As far as the influence of temperature is concerned, it can generally be claimed that higher temperatures enhance the singlet pathways, whereas lower temperatures make the triplet channel more favorable. Lowering of the temperature results in a diffusion-controlled decrease in the reaction from the singlet channel. The probability of the triplet reaction is less dependent on temperature because of the triplet lifetime, which is longer than that of singlet by about two orders of magnitude.

The activation barrier for the formation of the *exo*- product from the singlet channel is much smaller than for the formation of the *endo*- product. However, the pre-exponential factor for the *endo*- product is larger than for the *exo*- product. As the temperature decreases, the exponential part begins to dominate and more *exo*-product is formed.

The situation is completely different for the triplet pathway: the formation of both products has almost no barrier, whereas the pre-exponential factor favors the formation of the *endo*- product. When the triplet pathway predominates, the lack of the activation barrier results in the independence of stereoselectivity on the temperature.

Chapter 4

Experimental

4.1. Equipment

4.1.1. Measurements of EDL Spectral Characteristics

The spectral measurements were accomplished in a modified MW oven Whirlpool M401 (900 W), operating at 2450 MHz frequency and described by Literák and Klán [34], which had a window for UV radiation coming from EDL to a spectrometer. Its power was adjusted to the maximum in order to guarantee a continual MW irradiation. Every liquid is immediately boiling since EDL produces a considerable amount of IR radiation. The oven contained an external reflux condenser and a cooling glass spiral for removing redundant MW energy, thus preventing the magnetron from destruction by overheating [35,38].

The limit on the safe stray leakage of microwave power density was kept below 5 $mWcm^{-2}$ at 2450 MHz measured in the 50 mm distance from the equipment. The equipment was checked for leaks especially around the modified area [35].

Some experiments were carried out in a MW instrument Synthewave S 402 (300 W, Prolabo) equipped with an IR pyrometer, a quartz reaction vessel, and an external spiral reflux condenser).

The mercury EDLs were manufactured in Teslamp (Prague, Czech Republic). The lamps were made of a 9 or 14 mm quartz or Pyrex tubing (of approximately 1 mm

thick glass) of the 13 – 37 mm length, filled with mercury and argon, and sealed under 2.7 kPa vacuum [34]. The lamps filled with other materials and elements were manufactured in the Institute of Chemical Process Fundamentals, Academy of Sciences of the Czech Republic (V. Církva). They were made of Pyrex tubing (12 x 40 mm) and sealed in the argon atmosphere (0.7 kPa). Pyrex absorbs most of the UV radiation below 300 nm.

Gas chromatography was accomplished on a Shimadzu GC-2010 apparatus. The UV-VIS spectra of all chemicals were measured on a Shimadzu UV-1601 spectrophotometer.

4.1.2. Valerophenone and *p*-Nitroanisole Irradiation

The high-pressure irradiation experiments were carried out in MicroSYNTH microwave labstation (Milestone Microwave Laboratory Systems, Italy). The microwave apparatus contained a high-pressure Teflon reactor with an irradiated solution and an UVQ0007 electrodeless discharge lamp (12 x 85 mm, Milestone, Italy).

The irradiation of valerophenone and *p*-nitroanisole under atmospheric pressure was accomplished in a modified microwave oven Whirlpool M401 (900 W) with an opening on the side, facilitating the simultaneous MW heating and UV-irradiation from an external UV-light source (mercury lamp). For some experiments, the microwave instrument Synthewave S 402 was used.

Gas chromatography was accomplished on a Shimadzu GC-2010 gas chromatographer and on a Carlo Erba Strumentazione, HRGC 5160 apparatus, connected to a PC by a Perkin Elmer NCI 900 network chromatography interface.

4.2. Chemicals and Solvents

Methanol (pure) was obtained from ML Chemica and used as received. *n*-Pentane (pure) was purchased from Lachema and further purified by distillation. *n*-Hexane (SupraSolv) was bought from Merck and used as received. *n*-Heptane (pure) from Lachema was washed with concentrated sulfuric acid and distilled; *n*-decane (pure) from Reachim was washed with concentrated sulfuric acid and purified through an activated silica-gel column. Cyclohexane (pure) was obtained from Lach-Ner Co. The quality of all alkanes was checked by means of UV-VIS spectrophotometry and GC. The solvent absorbance values (vs. air) were negligible throughout the tested range of wavelengths (250 – 500 nm).

Valerophenone (>99 %) and hexadecane (99 %) were obtained from Aldrich Chemicals Co. Acetophenone (pure), *p*-nitrophenol (pure) and dichloromethane (pure) were purchased from Prolabo, NaOH (pure) and *p*-methoxyphenol (99 %) from Acros Organics. *p*-Nitroanisole was prepared from *p*-nitrophenol and dimethyl sulfate by a standard procedure and purified by recrystallization.

4.3. Spectral Measurements

A typical experimental system consisted of a quartz vessel containing a liquid and EDL, equipped with a reflux condenser, and placed to a microwave oven. The used AVS-S2000 spectrometer with an optic fiber probe served for measuring and evaluating the emission spectra using the software package AvaSoft (Avantes BV). The spectrum was recorded after the light source was stabilized. The effect of the output power of the MW reactor was investigated in the Synthewave S 402 MW instrument because its power (30 to 300 W) can be adjusted continuously, unlike that of domestic MW ovens.

4.4. Irradiation Procedures

4.4.1. Valerophenone

A high-pressure Teflon reactor containing the electrodeless discharge lamp, magnetic stirring bar and $5x10^{-5}$ mol of valerophenone (VP) dissolved in 50 ml of water was sealed, placed in the microwave apparatus and attached to its pressure and temperature sensors. A stirred mixture was first heated up by microwaves at low MW-output power (125 W) - the power of 125 W was too low to induce a discharge in the lamp but, at the same time, sufficient to heat up the mixture up to 160 – 170 °C.

When the temperature reached the desired level, the MW output power was increased to 300 – 400 W, which consequently resulted in the ignition of EDL. The irradiation was interrupted after 3 – 20 seconds. The reaction mixture was then cooled down, valerophenone, acetophenone and cyclobutanols were extracted into dichloromethane and analyzed on GC using hexadecane as an internal standard.

Experiments carried out under atmospheric pressure were accomplished both in a modified domestic MW oven and in the Synthewave S 402 microwave instrument. Quartz reaction vessels containing 30 ml of 0.001 M VP solution in cyclohexane and the electrodeless discharge lamp were placed in the domestic MW oven or in the S 402 MW instrument, respectively, and the MW output power was set to the maximum (900 W for the Whirlpool M401 MW oven; 300 W in the case of S 402 instrument). Samples were irradiated for 3 to 5 minutes and then analyzed by means of gas chromatography using hexadecane as an internal standard.

4.4.2. *p*-Nitroanisole

Both the experimental arrangement and the procedures used were similar to those employed in valerophenone photochemical experiments. The irradiated water solution contained $1x10^{-4}$ mol of *p*-nitroanisole and $1x10^{-2}$ mol NaOH. After the irradiation, the basic solution was neutralized/acidified by 1 M water solution of HCl, extracted into dichloromethane and analyzed on GC.

Several atmospheric pressure experiments were also carried out in a modified domestic microwave oven. One set of *p*-nitroanisole samples ($2x10^{-4}$ mol of *p*-nitroanisole in 30 ml of 0.01 M aqueous NaOH) was irradiated by an external UV-light source under simultaneous MW heating for 20 minutes. The other set was only heated for the same period of time so that both photochemical and possible thermic reaction pathways could be determined and compared.

Chapter 5

Results and Discussion

5.1. Emission Characteristics of Electrodeless Discharge Lamps (see Appendix)

5.1.1. Effects of Temperature

The temperature-dependent emission spectra of Hg-EDL were determined in various UV-transparent hydrocarbons with boiling points ranging from 35 to 174 °C (*n*-pentane, 35 °C; *n*-hexane, 69 °C; *n*-heptane, 98 °C; *n*-decane, 174 °C), which guaranteed a constant cooling of the lamp. The lamp temperature was, however, expected to be somewhat higher than that of the solvent.

Fig. 5.1. Emission spectra of EDL in several *n*-alkanes (boiling points).

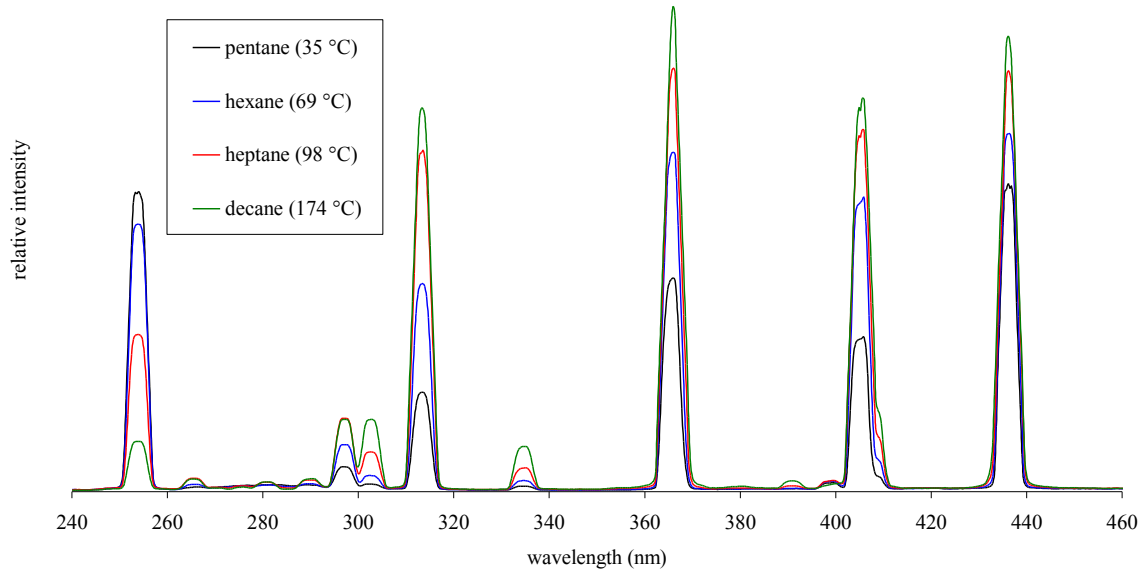

The relative emission peak intensity changes in *n*-pentane, *n*-hexane, *n*-heptane and *n*-decane are shown in Fig. 5.1. It is demonstrated that the relative intensity of the 254 nm band is highly dominant at a lower temperature in *n*-pentane while this band is negligible in *n*-decane.

At the same time, the 313 nm band becomes a principal wavelength in the UV region, which is well consistent with the above-described facts. The change of the solvent in a photochemical experiment would therefore dramatically influence the course of the reaction.

Figures 5.2 and 5.3 show a series of relative peak intensities (normalized on the 254 nm peak) at temperatures ranging from 35 to 174 °C for two differently sized quartz EDLs (9 x 13 mm and 14 x 37 mm). The spectra of both lamps present similar dependencies. Generally, the short wavelengths (especially the 254 nm peak) are distinctly suppressed with increasing temperature, whereas the longer wavelengths (over 300 nm) intensify.

Fig. 5.2. Temperature dependence of normalized emission bands in a 9 x 13 mm EDL.

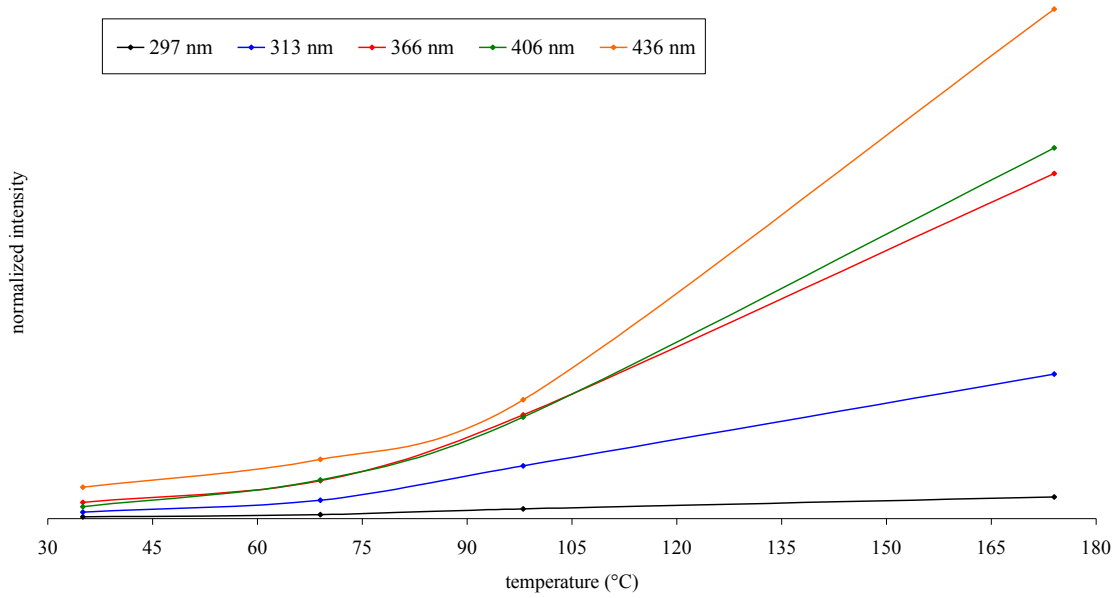

Fig. 5.3. Temperature dependence of normalized emission bands in a 14 x 37 mm EDL.

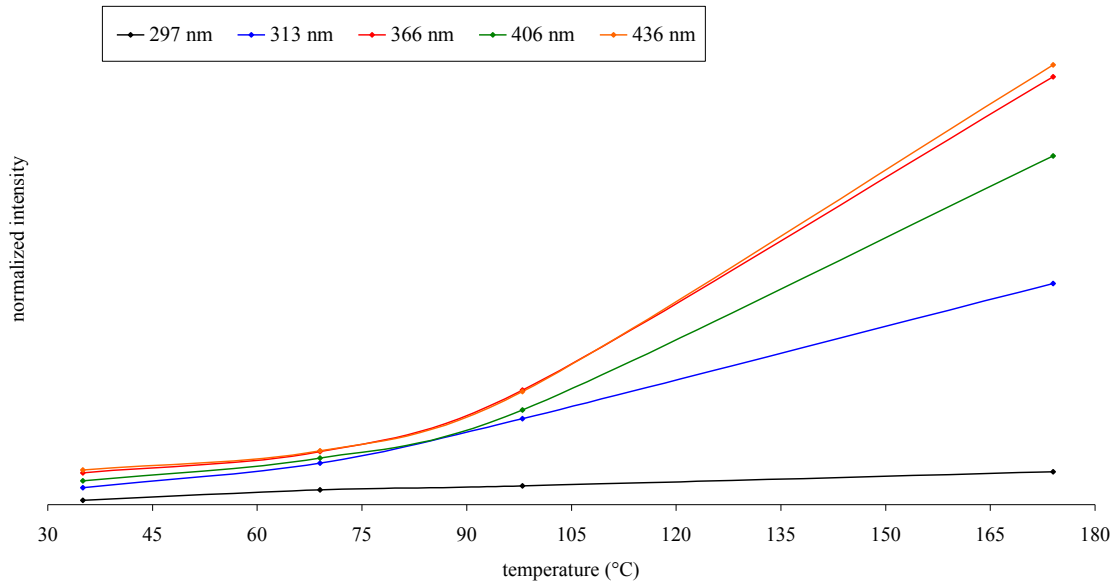

5.1.2. Effects of MW Output Power

The effect of the MW reactor output power was already investigated in the preliminary paper of Literák and Klán describing its influence on the Norrish type II reaction efficiency [34]. It was found that the reaction conversion increased in line with the increasing MW power, which boosted the UV irradiance. Fig. 5.4 shows the emission spectra of a quartz Hg-EDL at four different output power values (30, 120, 210 and 300 W). Relative peak intensities were more or less the same and their dependencies on the power are shown in Fig. 5.5.

All values increased linearly at small power values and then leveled off. This means that the emission efficiency of the lamp has been saturated at 200 W output power and EDL was not able to accept more MW energy (that was then dissipated to the environment). For routine experiments with EDLs, such an optimization of the power/emission efficiency ratio is highly recommended.

Fig. 5.4. Emission spectra of a quartz Hg-EDL at 30, 120, 210 and 300 W output power.

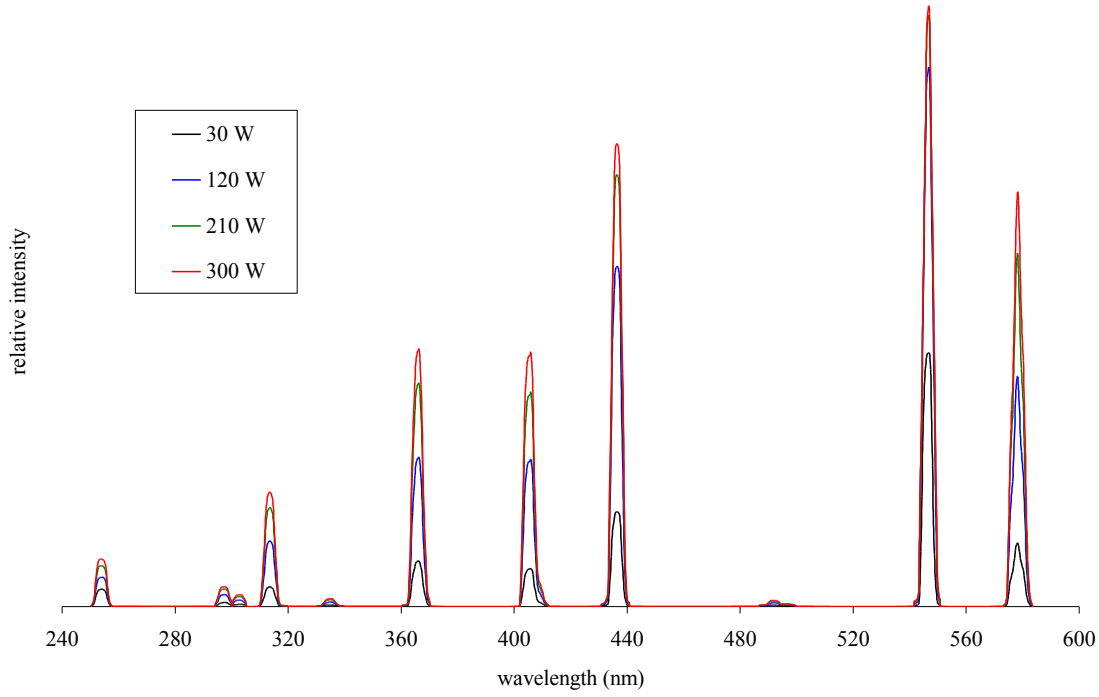

Fig. 5.5. Output power dependence of the emission bands (quartz EDL, Synthewave).

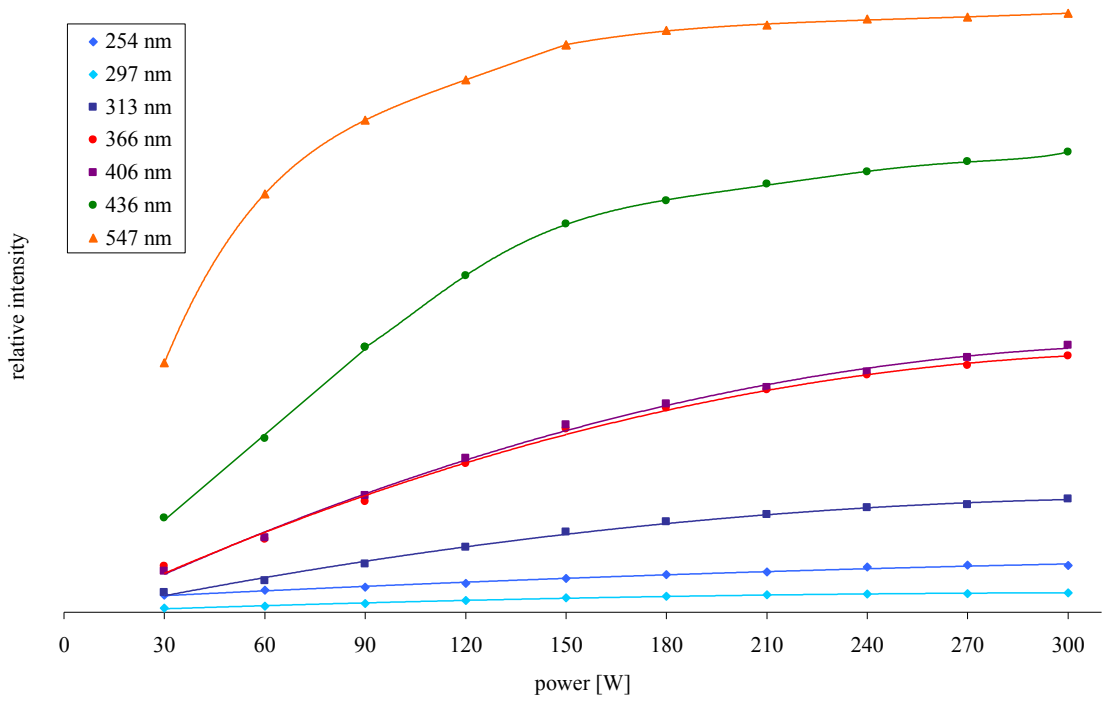

The output power of a commercially available MW oven can be lowered by cooling water in the tube inside the cavity [35]; however, it had only minor effect on the lamp emission efficiency in these experiments.

A solvent, which absorbs MW radiation, reduced the intensities of all emission bands since it reduces the amount of MW energy that powers the lamp. The EDL spectrum in methanol (bp = 65 °C) is compared to that in *n*-hexane (bp = 69 °C) in Fig. 5.6. The actual temperature of methanol could be little higher due to the superheating effect [38] (see also Subchapter 1.3.1).

Fig. 5.6. Comparison of the emission spectra of a quartz EDL in hexane and methanol.

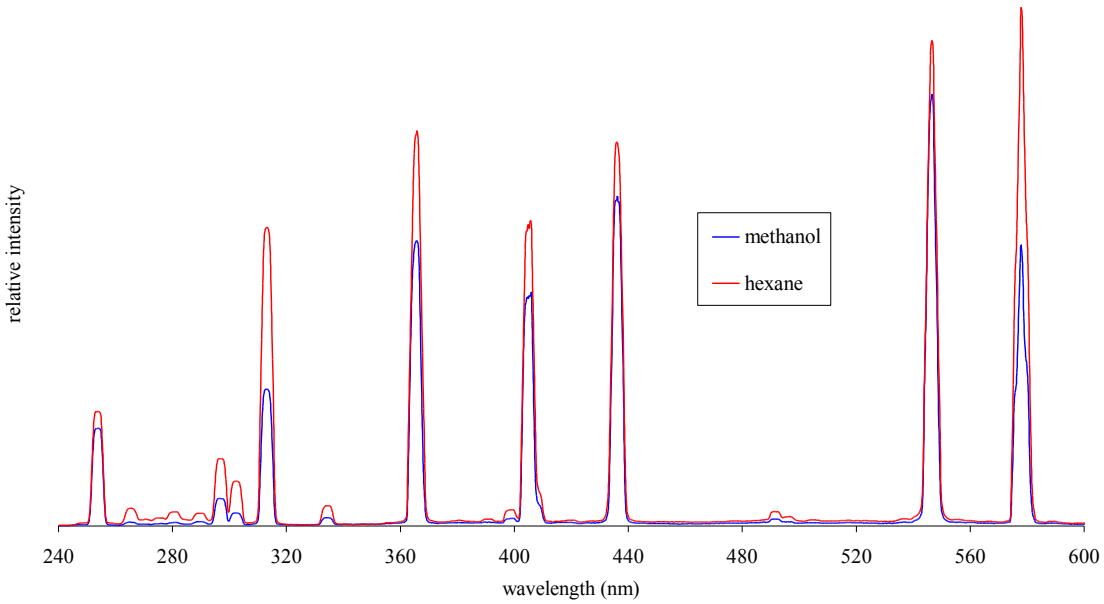

5.1.3. Effects of Solvent and EDL Envelope Material

Comparative conventional irradiation experiments with either quartz or Pyrex Hg-EDLs were already presented in the work of Klán and coworkers [34]. The conversion of valerophenone in the Norrish type II reaction was lowered when

a Pyrex Hg-EDL was used, which was explained by filtering off the part of the UV radiation. Fig. 5.7 shows a comparison of the emission spectra of quartz and Pyrex Hg-EDLs.

The Pyrex glass completely removes the 254 and 297 nm bands, however, the intensities of the remaining bands are virtually the same for both EDL envelope materials. The disappearance of the short wavelength bands well explains the efficiency loss observed in photochemical experiments using Pyrex instead of quartz lamps as sources of UV radiation.

Fig. 5.7. A comparison of the emission spectra of quartz and Pyrex EDLs in *n*-hexane.

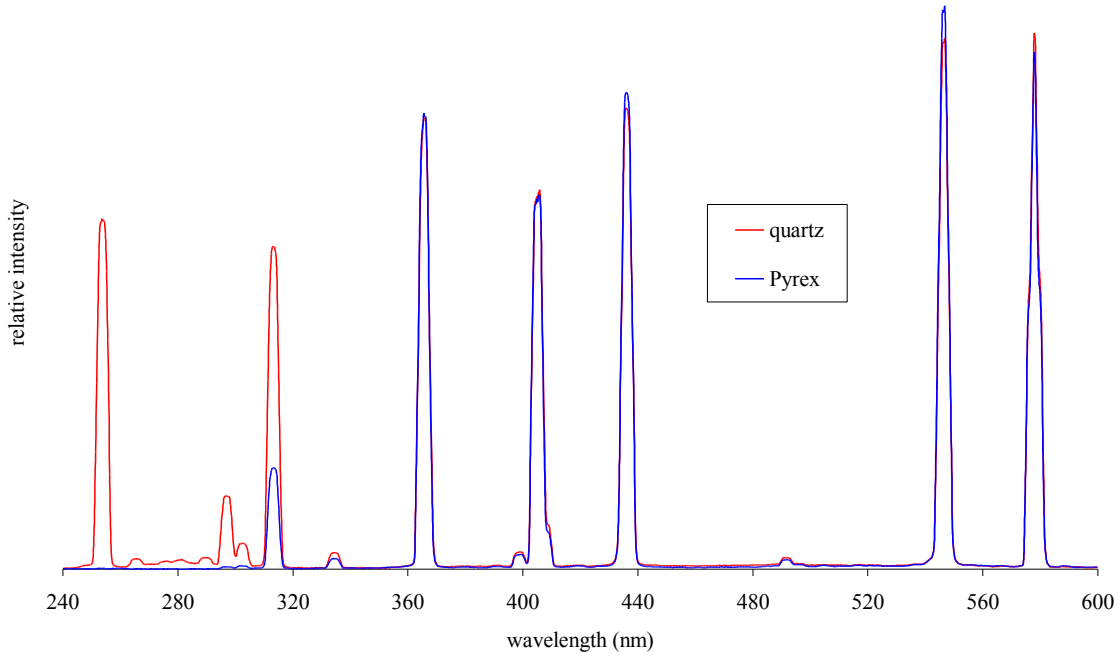

The solvent can also be used as an internal UV filter. Benzene, for example, significantly suppressed the wavelengths below 280 nm (Fig. 5.8). Therefore, *n*-hexane or other solvents, that are transparent over 220 nm, are to be used in case a short-wavelength irradiation is required.

Fig. 5.8. A comparison of the emission spectra of a quartz EDL in hexane and benzene.

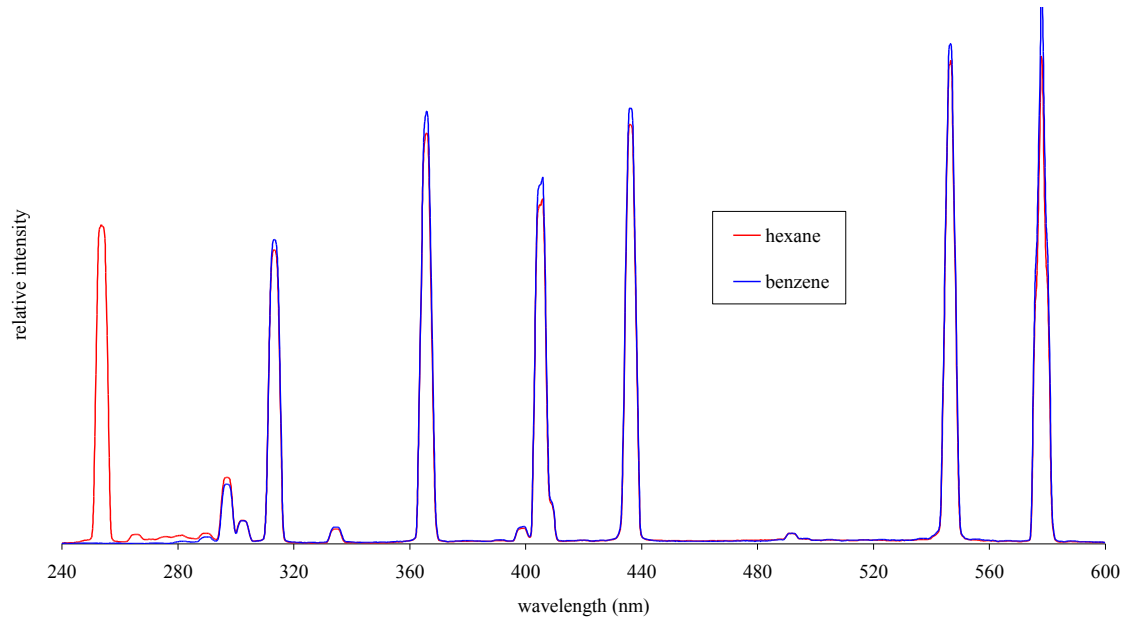

5.1.4. EDLs Filled With Other Elements/Materials

Spectral characteristics of EDLs containing additional filling materials were measured in *n*-decane (boiling point 174 °C). Fig. 5.9 shows spectrum of a quartz EDL filled with iodine vapors. Thanks to comparatively broad bands in its spectrum, I_2-EDL seems to be relatively universal and applicable to reactions requiring photochemical initiation within a spectral range of 270 – 350 nm*. However, I_2-EDLs cannot be easily ignited and they also proved to be very unstable.

By contrast, lamps filled with potassium iodide (KI-EDLs) appear to be substantially more stable and their spectral characteristics are very similar to those of I_2-EDLs. Fig. 5.10 depicts spectral characteristics of a Pyrex-KI-EDL.

** In case of Pyrex envelopes, the spectral region in question would be naturally somewhat narrower (310 – 350 nm) due to a low transmittance of the Pyrex glass bellow 310 nm; compare Fig. 5.9 and Fig. 5.10.*

Fig. 5.9. Spectrum of a quartz EDL filled with iodine vapors.

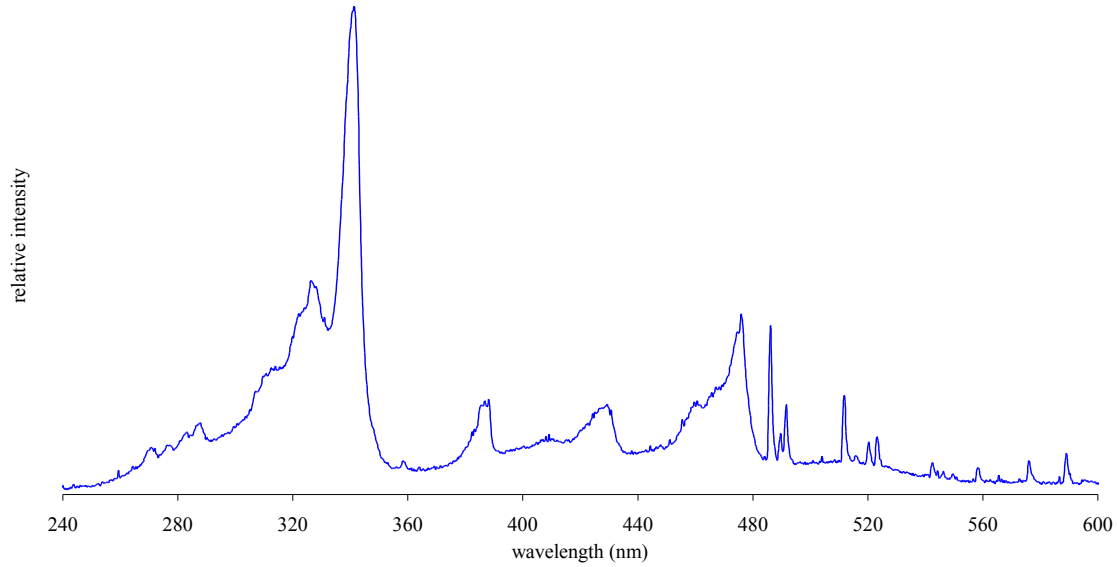

Fig. 5.10. Spectrum of a Pyrex EDL filled with 4 mg of KI.

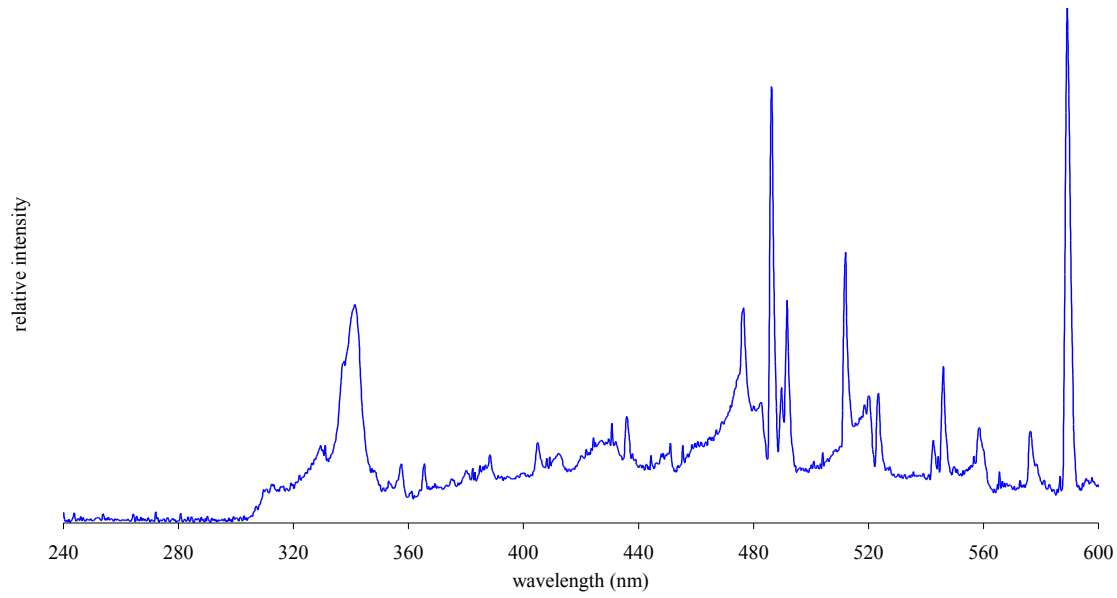

Figs. 5.11 and 5.12 depict spectra of Pyrex EDLs filled with different amounts of phosphorus. Spectra of both lamps contain distinct emission bands in the region between 341 and 343 nm. The bands at 325 and 327 nm are to be found only in

the spectrum of the lamp filled with 1 mg of phosphorus. On the other hand, the lamp containing 10 mg of P has a bit more multifarious emission spectrum in the VIS region.

A relative diminishment of peaks at shorter wavelengths in line with an increasing amount of the filling material (thus in line with an increasing pressure) fully corresponds to the general trend (e.g. differences between emission spectra of high-pressure and low-pressure discharge lamps), which is also apparent from Figs. 5.1 – 5.3.

EDLs filled with phosphorus proved to be very stable even at temperature as high as the boiling point of decane (174 °C).

Fig. 5.11. Spectrum of a Pyrex EDL filled with 1 mg of phosphorus.

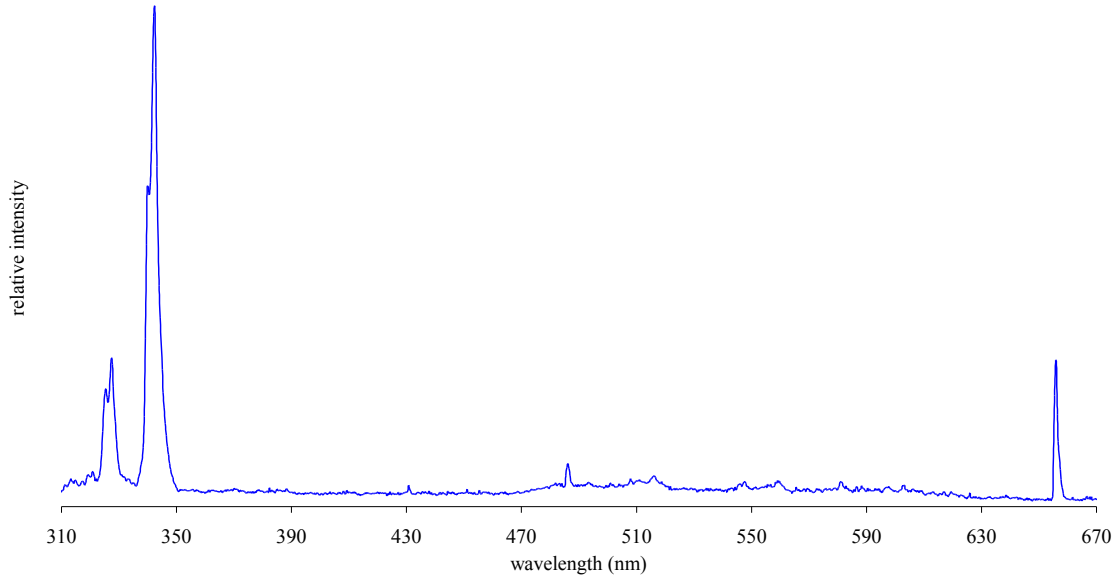

Fig. 5.12. Spectrum of a Pyrex EDL filled with 10 mg of phosphorus.

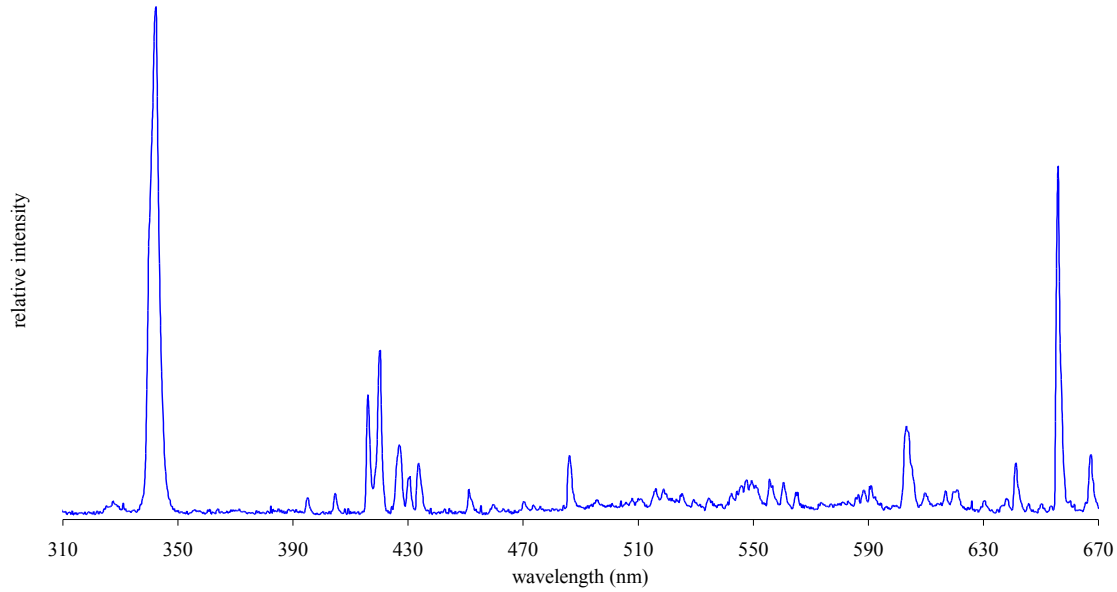

EDLs filled with selenium were relatively stable but their emission spectra containing virtually no significant bands in the UV region (Fig. 5.13), and especially the low intensities of the emitted radiation, indicate that the application of selenium EDLs in photochemical experiments is somewhat limited.

Fig. 5.13. Spectrum of a Pyrex EDL filled with 2 mg of selenium.

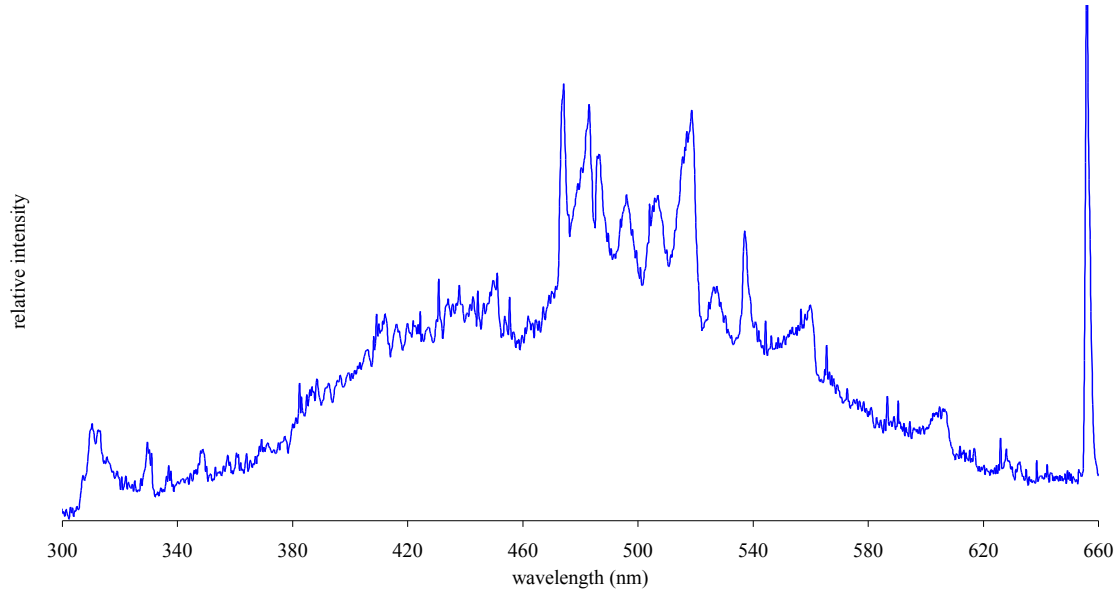

Unlike Se-EDLs, EDLs filled with sulfur seem to be predetermined for use in numerous reactions. The emission spectra of S-EDLs are virtually continuous and cover a broad range of wavelengths in the UV/VIS region (e.g. 310 – 570 nm in case of a Pyrex EDL containing 3 mg of sulfur, Fig. 5.14).

Fig. 5.14. Spectrum of a Pyrex EDL filled with 3 mg of sulfur.

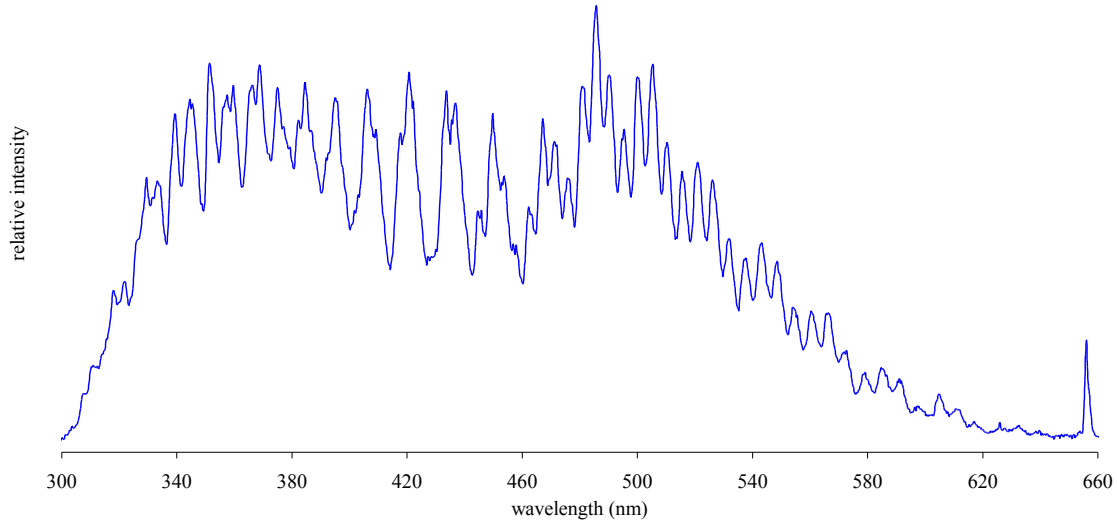

Fig. 5.15. Spectrum of sunlight [54].

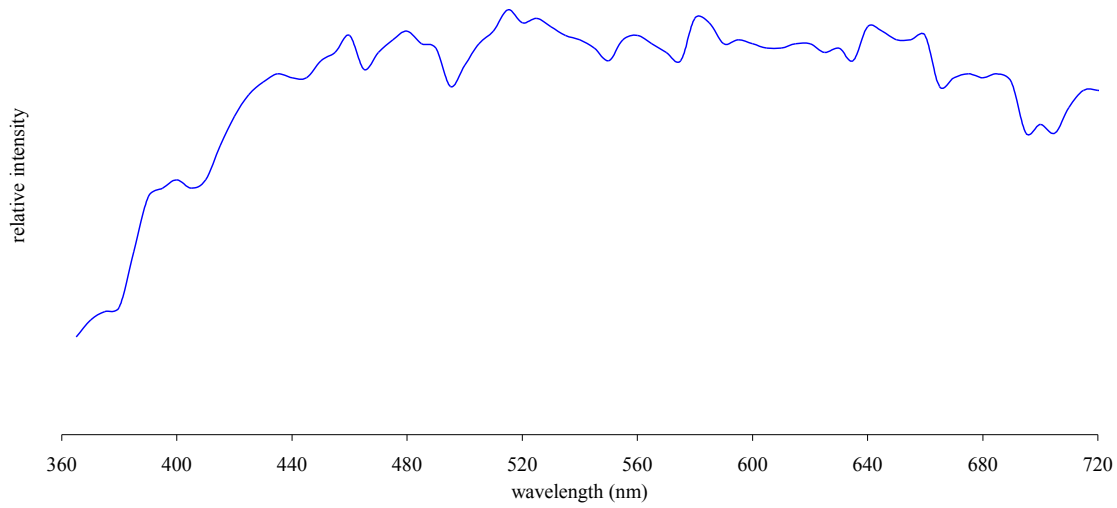

It was postulated in this subchapter that the intensities of the spectral bands are pressure- and temperature-dependent. The emission bands of S-EDLs found in the literature range from 350 to 850 nm [55–57]. The data from the literature together with Figs. 5.14 and 5.15 indicate that by optimizing the amount of sulfur in the lamp and the temperature of the ambient reaction system, one could easily and relatively well simulate the sunlight radiation using sulfur lamps. The sulfur EDLs thus seem to be predetermined for various environmental applications, such as investigation of photochemical transformations of both organic and inorganic environmental pollutants induced by sunlight radiation, etc.

5.2. EDL Fill and the Efficiency of Type II Photoreaction

0.001 M solution of valerophenone in cyclohexane (B.p. 80.7 °C) was subjected to irradiation by four different Pyrex EDLs (of the same size) filled with sulfur (0.5 mg), selenium (2.0 mg), phosphorus (2.0 mg), and mercury (1.0 mg), respectively. Experiments were accomplished both in the modified domestic MW oven and in the Synhewave S 402 apparatus. The irradiation times ranged from 3 to 5 minutes and the maximum overall VP conversions did not exceed 20 %.

Table 5.2. Overview of VP conversion rates for individual EDLs and MW devices.

EDL	Conversion Rate (% / min)	
Filling Material	Domestic MW Oven	Synthewave S 402
sulfur	2.60	5.09
selenium	0.20	0.87
phosphorus	1.71	2.09
mercury	0.40	0.81

Table 5.2 clearly illustrates the influence of MW field intensity on the EDL performance. All tested EDLs demonstrated a better stability and higher emission

efficiency when powered by focused microwaves (S 402). This influence was most pronounced in the case of selenium EDL. By contrast, the performance of phosphorus EDL was almost the same in both MW devices. However, it was already mentioned in Subchapter 5.1.4 that P-EDLs mark out by high emission stability (even when powered by unfocused microwaves in the modified domestic MW oven).

The highest conversion rate in both domestic MW oven and the Synthewave S 402 instrument was reached with the sulfur EDL. S-EDL proved to be somewhat unstable in the domestic MW oven but its performance in the S 402 instrument was satisfactory. For the possible applications (see Subchapter 5.1.4), use of a source of homogenous MW field is highly recommended.

5.3. Chemistry in Superheated Water

The value of relative permittivity ε_r (also called dielectric constant) of most materials, as established in the Subchapter 1.2, is greatly dependent on their actual temperature. The relative permittivity of a substance/solvent is large if its molecules are polar or highly polarizable [3]. In other words, the relative permittivity is a parameter characteristic of solvent polarity [58].

The synthetic chemists all over the world have been striving to limit the use of dangerous organic solvents and looking for more environment-friendly alternatives. The so-called ”solvent-free” experiments/procedures (e.g. taking advantage of the solid matrix such as alumina, silica, etc.) can rarely evade the use of organic solvents at least during the subsequent isolation procedures.

The attempts to use water as a solvent for organic reactions seem to be predetermined to failure because of the low water-solubility of most organic compounds. Nevertheless, it is known that the value of water relative permittivity (78 at room

temperature) decreases in line with increasing temperature, reaching the value of e.g. acetonitrile permittivity (i.e. 37) at temperatures around 180 °C [4]. This means that even some relatively non-polar organic compounds can dissolve in water and readily react with each other in solution, supposing the temperature is high enough. Arising products and the rest of reactants can then be simply isolated by cooling down the reaction mixture and by subsequent filtration or separation.

It is obvious that superheated water might in many cases substitute for organic solvents. This is also demonstrated on the following photochemical experiments.

5.3.1. Photochemistry of Valerophenone

Valerophenone undergoes the Norrish Type II photoreaction (see Subchapter 3.1) yielding products of fragmentation (acetophenone and propene) and Yang cyclization (cyclobutanols).

A set of irradiation experiments was carried out in order to investigate the behavior of valerophenone in water under extreme conditions. Several experiments with (10- to 100-times) higher amounts of valerophenone were also performed in order to verify a possible dependency of fragmentation/cyclization (F/C) ratio on the valerophenone concentration and to report on the potential synthetic use (the Norrish Type II photoreactions can be used for preparation of compounds, which cannot be easily prepared by traditional synthetic methods).

The acquired F/C ratios (Table 5.1) were plotted against temperature and fit by a smooth curve (Fig. 5.16). The F/C ratio proved to be independent on valerophenone concentration, as well as on its conversion. The ratio, however, appeared to be dependent on the temperature of the reaction mixture. The F/C ratio increased in line with the raising temperature. High temperatures enhanced the fragmentation at the expense of

cyclization, presumably by lowering the energy barrier hindering the cleavage of C_α-C_β bond. As far as the synthetic viewpoint is concerned, it can be claimed that the higher the temperature, the less favorable conditions for the preparation of cyclobutanols.

Relatively small conversions of valerophenone in the case of experiments with higher concentrations were most probably due to the so-called "internal filter effect" (i.e. most of the UV-radiation emitted by the EDL was absorbed by VP molecules in the immediate vicinity of the lamp, which thus prevented the rest of molecules from collision with high-energy photons (thereby from their excitation and reaction).

Table 5.1. Summary of the experimental conditions and the obtained results for irradiation of $5x10^{-5}$ mol VP in 50 ml of water.

Temperature (°C, average)	Time (sec)	Pressure Range (bar)	Conversion (%)	Ratio F/C
101*	20	1.0 – 1.3	16.7	4.52
104*	10	1.0 – 1.3	9.9	4.75
106	3	1.1 – 1.2	22.4	4.80
107	3	1.2 – 1.3	14.9	4.69
107	10	1.0 – 1.3	41.5	4.76
108	15	1.1 – 1.3	29.8	4.78
109	10	1.2 – 1.4	38.5	4.89
110	20	1.2 – 1.3	37.7	4.78
117	15	1.4 – 2.7	70.2	5.20
128	15	2.0 – 3.4	66.9	5.47
131**	490	1.0 – 3.0	26.3	5.58
142	15	4.0 – 6.2	86.5	5.66
157	10	6.0 – 7.8	79.0	6.09
168	10	7.1 – 9.1	65.5	6.35
196	6	18.7 – 22.0	64.6	6.81

** $5x10^{-4}$ mol VP; ** $5x10^{-3}$ mol VP).*

Fig. 5.16. Fragmentation/cyclization ratio plotted against average temperature of the mixture during irradiation.

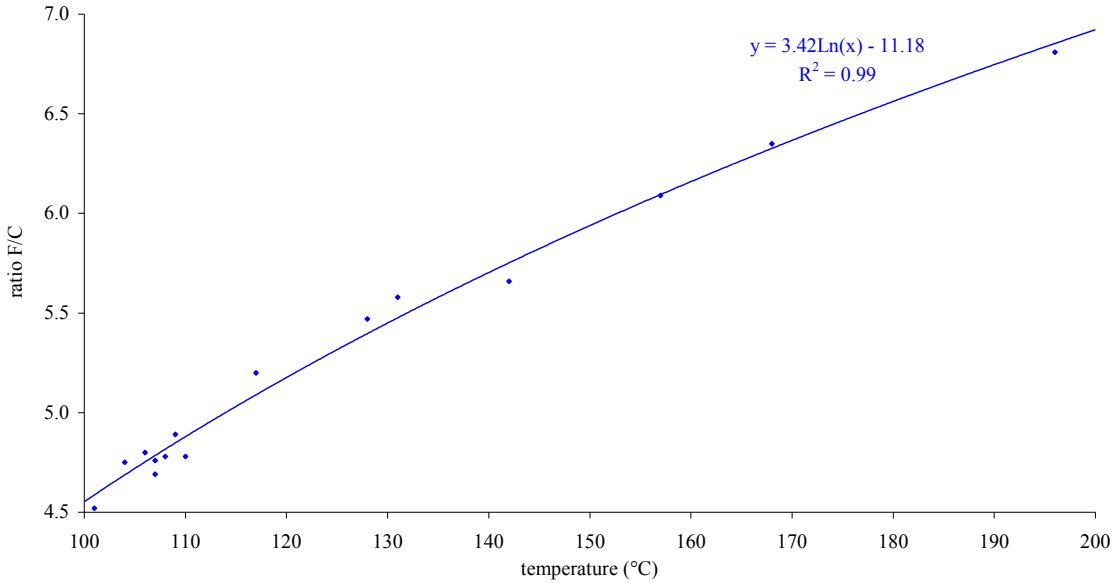

Fig. 5.17. F/C ratio plotted against reciprocal temperature values (1000/T).

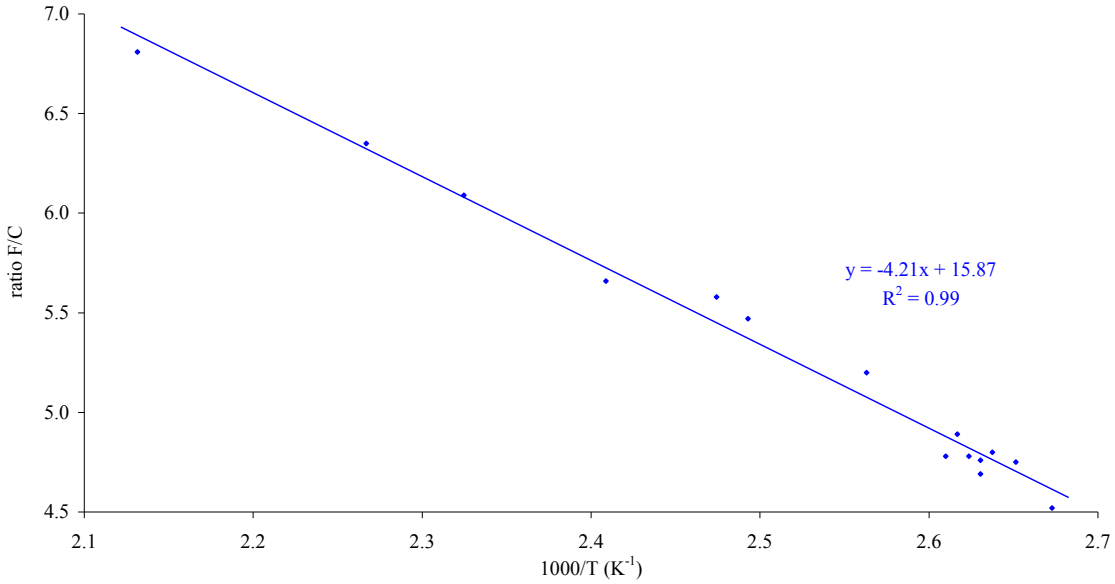

5.3.2 Photochemistry of 4-Nitroanisole

High-Pressure Experiments (EDL, Milestone Microwave Instrument)

The photosubstitution reaction of 4-nitroanisole with the OH^- ion cannot be easily predicted. The main products were reported by Letsinger and coworkers [59] and Havinga and de Vries [60] to be 4-methoxyphenols and 4-nitrophenols. The formation of 4-methoxyphenols is in agreement with the orientation rule for an electron donating substituent [60] but the mechanism of the 4-nitrophenol formation is still unclear.

While the irradiation of 4-nitroanisole in basified solutions of aliphatic alcohols resulted in a formation of two photoproducts [40], only one product – 4-nitrophenol – was observed in water (Scheme 5.1) at temperatures ranging from 95 to 170 °C. Furthermore, this product surprisingly arose even in the absence of UV light and microwaves, though in somewhat smaller amount. Klán et al. [40] observed no "dark photochemistry" when aliphatic alcohols were used as solvents.

Scheme 5.1.

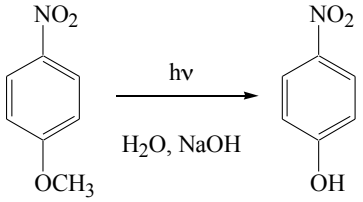

Two almost identical experiments (identical amounts of 4-nitroanisole, experimental arrangement, and time/temperature program) were carried out – one with EDL present in the reactor and the other without it. The heating of a 4-nitroanisole water solution with additional UV irradiation (60 seconds) resulted in ca 20 % conversion, while the experiment in the absence of EDL brought about only 15 % conversion.

The photochemical experiments carried out in the modified domestic MW oven under atmospheric pressure yielded both 4-nitrophenol and 4-methoxyphenol (Scheme 5.2, ratio about 1:1).

Scheme 5.2.

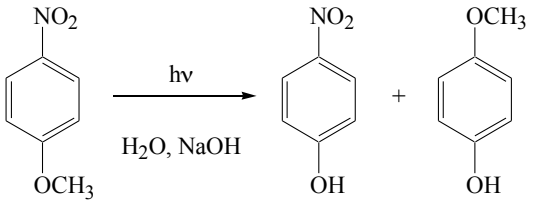

However, when the UV-light source was turned off and the mixture was heated solely by microwaves, no 4-methoxyphenol was formed and 4-nitrophenol was the only product obtained (Scheme 5.3). In addition to that, the conversion of 4-nitroanisole was smaller (by about 50 %) than that in the case of photochemical experiments (see Table 5.3).

Scheme 5.3.

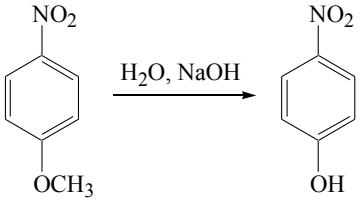

It could therefore be stated that the thermic reaction yields exclusively 4-nitrophenol, whereas the photochemical reaction pathway leads to the formation of both 4-methoxyphenol and 4-nitrophenol.

The possible explanation of why no 4-methoxyphenol was observed in the case of high-pressure experiments with EDL is that the irradiation times were too short and, apart from that, the vast majority of the 4-nitroanisole underwent thermic reactions

before the EDL was actually ignited and thus virtually no 4-methoxyphenol could be detected.

Table 5.3. Comparison of data from experiments carried out under atmospheric pressure.

Conditions	Time (min)	m_o nitroanisole (mg)	mol % methoxyphenol	mol % nitrophenol	mol % nitroanisole	mol % losses
MW	20	34.3	0.0	5.2	86.3	8.5
MW	20	34.8	0.0	4.4	88.8	6.8
MW	20	33.0	0.0	5.8	86.1	8.1
MW + UV	20	35.6	8.7	12.6	74.9	3.8
MW + UV	20	32.6	9.4	8.6	75.5	6.5
MW + UV	20	32.7	9.9	9.6	69.7	10.8

Conclusions

It was shown that the spectral output of the electrodeless discharge lamps depends on numerous factors such as temperature of the ambient environment, EDL envelope glass material, solvent used in a photochemical reaction, amount of the filling substance, and the intensity and the nature of the MW field.

Dependence of the EDL output power on the intensity of MW field may not be linear in the whole range of accessible MW field intensities, routine experiments with EDLs should therefore be preceded by optimization of the power/emission efficiency ratio.

Sulfur EDLs may potentially be used for simulation of sunlight radiation in the laboratory experiments.

Since the application of EDLs in photochemistry is very simple and accessible to a broad spectrum of chemists, it is likely to find its way into a conventional chemical laboratory.

The accomplished experiments with irradiation of valerophenone and 4-nitroanisole in superheated water indicate that superheated water may in many cases represent a reasonable alternative to environment-unfriendly organic solvents.

The experiments with 4-nitroanisole in water afforded surprising results. One of the usual photochemical products, 4-nitrophenol, was observed even in the absence of the UV radiation, thus under purely thermic conditions. This might be explained by a decrease in activation energy due to a different nature of solvation in the case of water molecules. However, the complete understanding of this phenomenon and of the mechanism of photochemical S_NAr as such still remains unanswered.

References

[1] R. N. Gedye, F. Smith, K. Westaway, Tetrahedron Lett. 27 (1986) 279.

[2] J. March, Advanced Organic Chemistry (1968).

[3] P. W. Atkins, Physical Chemistry, 6th Edition (1998) 654.

[4] J. A. Dean, Lange's Handbook of Chemistry, 13th ed., Mc Graw-Hill, New York (1985).

[5] L. Perreux, A. Loupy, Tetrahedron 57 (2001) 9199.

[6] D. R. Barghurst, M. P. Mingos, J. Chem. Soc., Chem. Commun. (1992) 674.

[7] R. A. Abramovich, Org. Prep. Proc. Int. 23 (1991) 683.

[8] A. L. Buchachenko, E. L. Frankevich, Chemical Generation and Reception of Radio- and Microwaves (1994).

[9] N. J. Turro, Modern Molecular Photochemistry (1991).

[10] A. V. Astashkin, Y. Sakaguchi, J. Chem. Phys. 106 (1997) 9190.

[11] J. R. Woodward, R. J. Jackson, C. R. Timmel, K. A. McLauchlan, P. J. Hore, Chem. Phys. Lett. 272 (1997) 376-382.

[12] D. V. Stass, J. R. Woodward, C. R. Timmel, P. J. Hore, K. A. McLauchlan, Chem. Phys. Lett. 329 (2000) 15-22.

[13] C. R. Timmel, J. R. Woodward, P. J. Hore, K. A. McLauchlan, D. V. Stass, Meas. Sci. Technol. 12 (2001) 635-643.

[14] C. R. Timmel, P. J. Hore, Chem. Phys. Lett. 257 (1996) 401-408.

[15] T. Ritz, S. Adem, K. Schulten, Biophys. J. 78 (2000) 707-718.

[16] Š. Toma, A. Gáplovský, J.L. Luche, Ultrason. Sonochem. 8 (2001) 201.

[17] A. Gáplovský, J. Donovalová, Š. Toma, R. Kubinec, Ultrason. Sonochem. 4 (1997) 109.

[18] A. Gáplovský, J. Donovalová, Š. Toma, R. Kubinec, J. Photochem. Photobiol. A Chem. 115 (1998) 13.

[19] H. Hayashi, Y. Sakaguchi, M. Wakasa, Bull. Chem. Soc. Jpn. 74 (2001) 773.

[20] J. R. Woodward, Prog. React. Kinet. Mech. 27 (2002) 165.

[21] P. Klán, V. Církva, Microwave photochemistry, in: A. Loupy (Ed.), Microwaves in Organic Synthesis, Wiley–VCH, Weinheim (2002).
[22] R. A. Abramovitch, Org. Prep. Proced. Int. 23 (1991) 685.
[23] D. M. P. Mingos, D. R. Baghurst, Chem. Soc. Rev. 20 (1991) 1.
[24] A. G. Whittaker, D. M. P. Mingos, J. Microw. Power Electromagn. Energy 29 (1994) 195.
[25] S. A. Galema, Chem. Soc. Rev. 26 (1997) 233.
[26] S. C. Brown, Introduction to Electrical Discharges in Gases, Wiley, New York, (1966).
[27] P. Spietz, U. Gross, E. Smalins, J. Orphal, J.P. Burrows, Spectrochim. Acta Part B At. Spectrom. 56 (2001) 2465.
[28] R. F. Browner, J. D. Winefordner, Spectrochim. Acta 28B (1973) 263.
[29] J. Sneddon, R. F. Browner, P. N. Keliher, J. D. Winefordner, D. J. Butcher, R. G. Michel, Prog. Anal. Spectrosc. 12 (1989) 369.
[30] N. Imamura, J. Sakaguchi, S. Asatani, S. Hashiguchi, K. Obara, J. Cryst. Growth 237 (2002) 76.
[31] J. P. S. Haarsma, G. J. DeJong, J. Agterdenbos, Spectrochim. Acta 29B (1974) 1.
[32] W. S. Gleason, R. Pertel, Rev. Sci. Instrum. 42 (1971) 1638.
[33] P. Klán, J. Literák, M. Hájek, J. Photochem. Photobiol. A Chem. 128 (1999) 145.
[34] J. Literák, P. Klán, J. Photochem. Photobiol. A Chem. 137 (2000) 29.
[35] P. Klán, M. Hájek, V. Církva, J. Photochem. Photobiol. A Chem. 140 (2001) 185.
[36] I. E. Den Besten, J.W. Tracy, J. Chem. Educ. 50 (1973) 303.
[37] V. Církva, M. Hájek, J. Photochem. Photobiol. A Chem. 123 (1999) 21.
[38] P. Klán, J. Literák, S. Relich, J. Photochem. Photobiol. A Chem. 143 (2001) 49.
[39] J. Literák, P. Klán, D. Heger, A. Loupy, J. Photochem. Photobiol. A Chem. 154 (2002) 155.
[40] P. Klán, R. Ruzicka, D. Heger, J. Literák, P. Kulhánek, A. Loupy, Photochem. Photobiol. Sci. 1 (2002) 1012.
[41] A. G. Howard, L. Labonne, E. Rousay, Analyst 126 (2001) 141.
[42] D. Florian, G. Knapp, Anal. Chem. 73 (2001) 1515.

[43] S. Horikoshi, H. Hidaka, N. Serpone, J. Photochem. Photobiol. A Chem. 153 (2002) 185.

[44] S. Horikoshi, H. Hidaka, N. Serpone, Environ. Sci. Technol. 36 (2002) 5229.

[45] F. W. McLafferty, Anal. Chem. 31 (1956) 82.

[46] P. J. Wagner, G. S. Hammond, J. Am. Chem. Soc. 88 (1966) 1245.

[47] P. J. Wagner, Acc. Chem. Res. 4 (1971) 168.

[48] P. Klán, Organická fotochemie (2001).

[49] P. J. Wagner, B.-S. Park, Organic Photochemistry 11 (1991) 227.

[50] P. Klán, J. Literák, Collect. Czech. Chem. Commun. 64 (1999) 2007.

[51] J. Cornelisse, CRC Handbook of Org. Photochem. Photobiol., CRC Press, Boca Raton (1995).

[52] A. G. Griesbeck, S. Bondock, M. S. Gudipati, Angew. Chem. Int. Ed. 40, No. 24 (2001) 4684.

[53] J. Kossanyi, S. Sabbah, P. Chaquin, J.C. Ronfart-Haret, Tetrahedron 37 (1981) 3307.

[54] L. I. Grossweiner, The Science of Photobiology, 2nd Edition (1989).

[55] J. T. Dolan, M. G. Ury, C. H. Wood, U.S. Pat. Appl. (1995) US 5404076.

[56] D. A. Kirkpatrick, J. T. Dolan, D. A. MacLennan, B. P. Turner, J. E. Simpson, PCT Int. Appl. (2000) WO 0070651.

[57] M. Kamarehi, L. Levine, M. G. Ury, B. P. Turner, U.S. Pat. Appl. (1998) US 5831386.

[58] G. Wypych, Handbook of Solvents (2001) 55.

[59] R. L. Letsinger, O. B. Ramsey, J. H. McCain, J. Am. Chem. Soc. 87 (1965) 2945.

[60] S. de Vries, E. Havinga, Trav. Chim. Pays-Bas 84 (1965) 601.

Appendix

Available online at www.sciencedirect.com
SCIENCE DIRECT®
Journal of Photochemistry and Photobiology A: Chemistry 158 (2003) 1–5
Journal of Photochemistry and Photobiology A:Chemistry
www.elsevier.com/locate/jphotochem

The electrodeless discharge lamp: a prospective tool for photochemistry Part 4. Temperature- and envelope material-dependent emission characteristics

Pavel Müller[a], Petr Klán[a,*], Vladimír Církva[b]

[a] *Department of Organic Chemistry, Faculty of Science, Masaryk University, Kotlarska 2, 611 37 Brno, Czech Republic*
[b] *Institute of Chemical Process Fundamentals, Academy of Sciences of the Czech Republic, Rozvojova 135, 165 02 Prague 6, Suchdol, Czech Republic*

Received 12 February 2003; received in revised form 12 February 2003; accepted 20 February 2003

Abstract

This work extends our previous research on an original photochemical reactor—the electrodeless discharge lamp (EDL) inside a reaction mixture that generates ultraviolet radiation in the microwave (MW) field. This arrangement was found to be a straightforward solution for homogeneous as well as heterogeneous photochemical experiments that need to be carried out at higher temperatures. Here, we report the emission characteristics (250–600 nm) of EDL as a function of temperature, MW output power of the reactor, EDL envelope material, and properties of solvents used in photochemical reactions. Relative intensities of the individual emission peaks were found to be largely dependent on temperature (in the region of 35–174 °C): the short-wavelength bands (particularly the 254 nm peak) were suppressed with increasing temperature. Solvents absorbing MW significantly reduced the EDL emission intensity. It is concluded that the right choice of EDL envelope material and reaction conditions is essential for an efficient course of a photochemical process in this experimental arrangement.

Keywords: Photochemistry; Microwave; Electrodeless discharge lamp; Emission; Spectra

1. Introduction

There have been attempts to affect photochemical reactions by other sources of non-classical activation, such as ultrasound [1–3] or magnetic field [4,5]. Photochemistry in the microwave (MW) field [6] presents a combined chemical activation by two distinctive kinds of electromagnetic radiation. Energy of MW radiation ($E = 0.4$–$40\,\mathrm{J\,mol^{-1}}$ at $\nu = 1$–$100\,\mathrm{GHz}$) is considerably lower than that of UV-Vis radiation ($E = 600$–$170\,\mathrm{kJ\,mol^{-1}}$ at $\lambda = 200$–$700\,\mathrm{nm}$), thus insufficient to disrupt bonds of common organic molecules. Microwave heating is not identical to classical external heating, at least at the molecular level [7–10]. Molecules with a permanent (or induced) dipole respond to an electromagnetic field by rotating, which results in friction with neighboring molecules (thereby in heat). There are some additional (secondary) effects of microwaves, including ionic conduction (ionic migration in the presence of an electric field) or spin alignment. Therefore, MW effects on photochemical reactions are expected to be diverse.

The objective of photochemistry in the microwave field is frequently, but not irreplaceably, connected to the electrodeless discharge lamp (EDL), which generates UV radiation when placed into the MW field. We have reported on an original photochemical reactor that takes advantage of an EDL *inside* a reaction mixture (Fig. 1) [11–13]. Such an arrangement was proposed for the first time by Den Besten and Tracy [14], and later applied by Církva and Hájek [15] in experiments using a modified microwave oven. Photochemical applications of a microwave-powered light source in photochemistry were recently described in several articles [16–22]. Knowledge of spectral characteristics of EDL is clearly essential for planning the photochemical experiment. The right choice of a filling and envelope material, glass, and even temperature can dramatically modify the emission spectrum. In the present study, we describe the influence of the EDL properties, the MW output power, and the reaction conditions on the EDL spectral characteristics.

* Corresponding author. Tel.: +420-5-41129356; fax: +420-5-41129641.
E-mail address: klan@sci.muni.cz (P. Klán).

1010-6030/03/$ – see front matter © 2003 Elsevier Science B.V. All rights reserved.
doi:10.1016/S1010-6030(03)00101-1

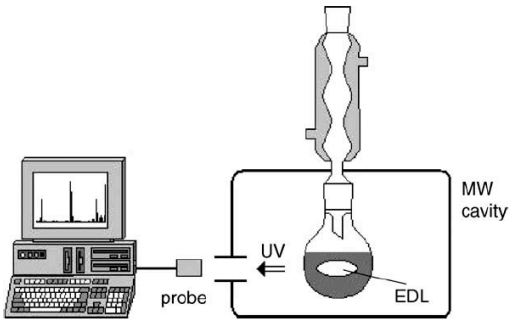

Fig. 1. Photochemistry in the MW field (adapted according to Klán et al. [13]).

2. Experimental

2.1. Equipment

The spectral measurements were accomplished in a modified MW oven Whirlpool M401 (900 W), operating at 2450 MHz frequency and described elsewhere [12], which had a window for UV radiation coming from EDL to a spectrometer. Its power was adjusted to the maximum in order to guarantee a continual MW irradiation. Every liquid is immediately boiling since EDL produces a considerable amount of IR radiation. The oven contained an external reflux condenser and a cooling glass spiral for removing redundant MW energy, thus preventing the magnetron from destruction by overheating [13,17]. Some experiments were carried out in a MW instrument Synthewave 402 (Prolabo, equipped with an IR pyrometer, a quartz reaction vessel, and an external spiral reflux condenser). The limit on the safe stray leakage of microwave power density was kept below 5 mW cm^{-2} at 2450 MHz measured in the 50 mm distance from the equipment. The equipment was checked for leaks especially around the modified area [13].

Electrodeless discharge mercury lamps were manufactured in Teslamp (Prague, Czech Republic). The lamps were made of a 9 or 14 mm quartz or Pyrex tubing (of approximately 1 mm thick glass) of the 13–37 mm length, filled with mercury and argon, and sealed under 2.7 kPa vacuum [12]. Pyrex absorbs most of the UV radiation below 290 nm. Gas chromatography was accomplished on a Shimadzu GC-17A apparatus. The UV-Vis spectra of all chemicals were measured on a Shimadzu UV-1601 spectrophotometer.

2.2. Chemicals

Methanol (pure, ML Chemica Co.) was used as received. *n*-Pentane (pure, Lachema Co.) was further purified by distillation and *n*-hexane (SupraSolv, Merck) was used as received. *n*-Heptane (pure, Lachema Co.) was washed with concentrated sulfuric acid and distilled; *n*-decane (pure, Reachim) was washed with concentrated sulfuric acid and purified through an activated silica-gel column. The quality of all alkanes was checked by the UV-Vis spectrophotometry and GC. The solvent absorbance values (versus air) were negligible throughout the tested range of wavelengths (250–500 nm).

2.3. Spectral measurements

A typical experimental system consisted of a quartz vessel containing a liquid and EDL, equipped with a reflux condenser, and placed to a microwave oven. The AVS-S2000 spectrometer with an optic fiber probe served for measuring and evaluating the emission spectra using the software package AvaSoft (Avantes BV). The spectrum was recorded after the light source was stabilized. The effect of the output power of the MW reactor was investigated in the Synthewave 402 MW instrument because, unlike domestic MW ovens, its power (30–300 W) can be adjusted continuously.

3. Results and discussion

The electrodeless discharge lamp is a glass tube filled with an excitable substance and sealed under a reduced pressure or a noble gas. A high frequency electromagnetic field (radio frequency or MW, 300–3000 MHz) can trigger gas discharge causing the emission of electromagnetic radiation. This phenomenon has been studied for many years and was already well understood in the 1960s [23]. EDL is usually characterized by a higher emission intensity than that of the hollow cathode lamps, a lower contamination due to the absence of the electrodes, and a longer lifetime [6]. EDLs operate due to free electrons in the fill that are accelerated by the MW field energy. They collide with the gas atoms and ionize them to release more electrons (the "avalanche" effect). The energetic electrons collide with the heavy-atom particles present in the plasma, thus exciting them from the ground state to higher energy levels. The excitation energy is then released as the electromagnetic radiation with the spectral characteristics according to the composition of the fill. There are a number of operating parameters [6], which have been recognized as influencing the electrodeless discharge lamp performance, such as temperature, nature and pressure of the fill gas, choice of the fill material, dimensions of the lamp envelope, the nature and characteristics of the MW energy coupling device, and the frequency and intensity of the MW energy.

The effect of temperature on EDL is closely associated with the fill gas pressure. At room temperature ($T \approx 300$ K) the gas mixture in the lamp has a pressure of approximately 2.6 kPa (0.026 atm), while in an operation mode the temperature of the plasma is most likely between 700 and 1400 K, and the pressure about 1 MPa (10 atm) [24]. The plasma includes strong non-equilibrium states due to high-energy particles. The plasma pressure influences the characteristics

of the radiation; it affects the mean free path of the particles and their collisional cross-sections. Pressure thus affects the number of collisions per unit of time. Lower-state atoms, which are outside the plasma but still within the lamp volume, have a lower temperature than the emitting atoms within the plasma. Therefore, their absorption line profile is narrower than the emission line profile from the plasma [24]. The spatial distribution and relative concentrations of emitting and absorbing atoms critically depend on the partial pressure of the element within the discharge volume: the higher the partial pressure of the element, the more lower-state atoms exist outside the emitting plasma. Therefore, more self-absorbed and -reversed atomic lines result from the simultaneous presence of emitting atoms and lower-state atoms.

The effect of temperature on radiance from EDLs was already investigated [24–26]. It was found that the optimum operating temperature for the mercury fill is 42 °C (for 253.7 nm line, 6^1S_0–6^3P_1). The output is reduced when the temperature is beyond optimum. Operation at high power or high temperatures can increase the intensity but, at the same time, reduce the lifetime and also lead to a broadening of the atomic line profile due to self-absorption and -reversal effects. The temperature dependence of emission intensities from mercury atoms at steady state for lines 365, 405, 436, 546 and 579 nm was also investigated [27]. The increase of the line emission intensities above 37 °C is explained by a decrease of the activation energy of mercury atoms or ions and by reduction of the number of bonds of a mercury atom in plasma. The influence of the lamp cooling by air stream, that can cause a lamp emission instability, was also examined [28]. If the vapor pressure in EDL is too high, the discharge may be limited or even extinguished completely [29].

3.1. Effects of temperature

In this work, the temperature-dependent emission spectra of Hg-EDL were determined in various UV-transparent hydrocarbons with boiling points of 35–174 °C (*n*-pentane, 35 °C; *n*-hexane, 69 °C; *n*-heptane, 98 °C; *n*-decane, 174 °C), which guaranteed a constant cooling down of the lamp temperature. The lamp temperature was, however, expected to be somewhat higher than that of the solvent. The relative emission peak intensity changes in *n*-pentane and *n*-decane are shown in Fig. 2. It is demonstrated that the relative intensity of the 254 nm band is highly dominant at a lower temperature in *n*-pentane while this band is negligible in *n*-decane, at the same time the 313 nm band becomes a principal wavelength in the UV region, which is well consistent with the above-described facts. The change of the solvent in a photochemical experiment would therefore dramatically influence the course of the reaction. Figs. 3 and 4 show a series of *relative* peak intensities (normalized on the 254 nm peak) at temperatures from 35 to 174 °C for two differently sized quartz EDLs. The spectra of both lamps present similar dependencies. Generally, the short

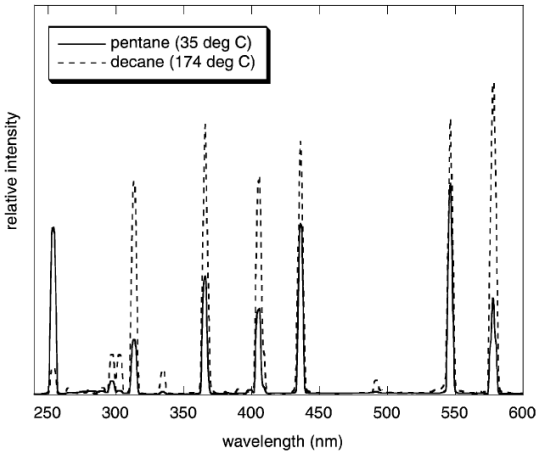

Fig. 2. Emission spectra of EDL in *n*-pentane and *n*-decane.

wavelengths (especially the 254 nm peak) are suppressed with increasing temperature.

3.2. Effects of the MW output power

The effect of the MW reactor output power was already investigated in our preliminary paper describing its influence on the Norrish type II reaction efficiency [12]. It was found that the reaction conversion increased with increasing MW power, which boosted the UV irradiance. Fig. 5 shows the emission spectra of a quartz Hg-EDL at two different output power values (30 and 300 W). Relative peak intensities were the same and their dependencies on the power are shown in Fig. 6. All values increased linearly at small power values and then leveled off. This means that the emission

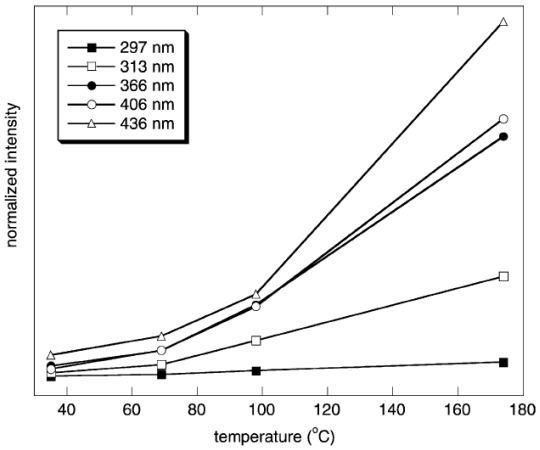

Fig. 3. Temperature dependence of the normalized emission bands in a 9 mm × 13 mm EDL.

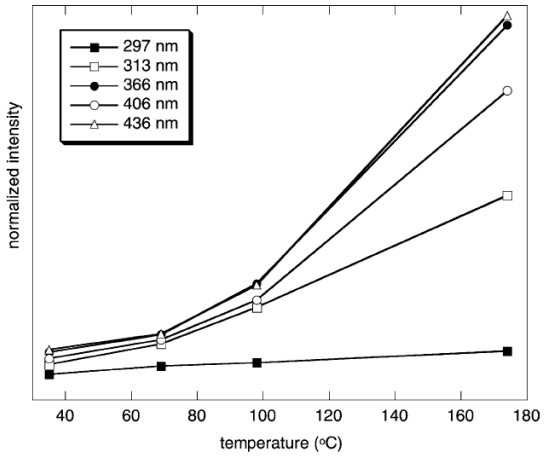

Fig. 4. Temperature dependence of the normalized emission bands in a 14 mm × 37 mm EDL.

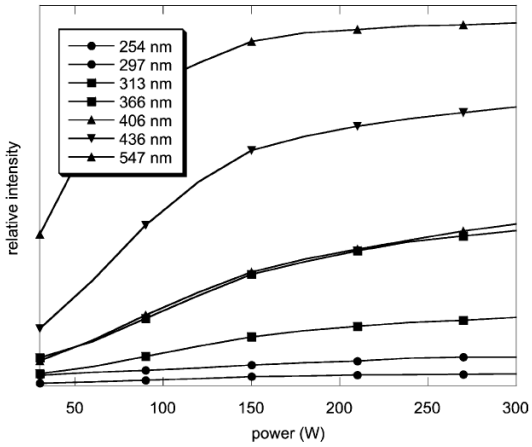

Fig. 6. Output power dependence of the emission bands (a quartz EDL; Synthewave 402).

efficiency of the lamp has been saturated at ~200 W power and EDL was not able to accept more MW energy (that was then dissipated to the environment). For routine experiments with EDLs, such an optimization of the power/emission efficiency ratio is highly recommended. The output power of a commercially available MW oven can be lowered by a cooling water in the tube inside the cavity [13], however, it had only minor effect on the lamp emission efficiency in our experiments.

A solvent, which absorbs MW radiation, reduced the intensities of all emission bands since it reduces the amount of MW energy that powers the lamp. The EDL spectrum in methanol (bp = 65 °C) is compared to that in hexane (bp = 69 °C) in Fig. 7. The actual temperature of methanol could be little higher due to the superheating effect [17].

3.3. Effects of the EDL envelope material and solvents

Comparative conventional irradiation experiments with either quartz or Pyrex Hg-EDLs were already presented in our previous work [12]. The conversion of valerophenone in the Norrish type II reaction was lowered when a Pyrex Hg-EDL was used, which was explained by filtering off the part of the UV radiation. Fig. 8 shows a comparison of the emission spectra of quartz and as Pyrex Hg-EDLs. The Pyrex glass completely removed the 254 and 297 nm bands, however, the intensity of the remaining bands was the same. This

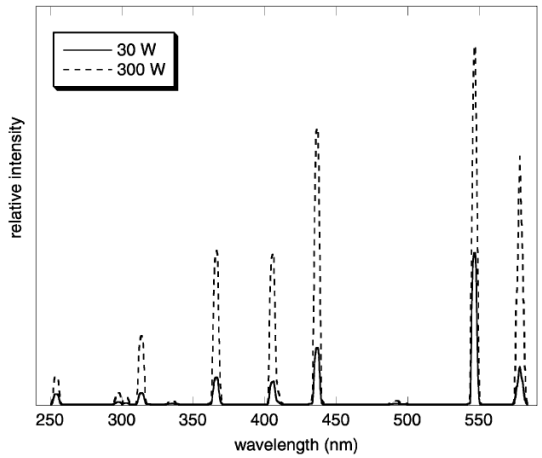

Fig. 5. Emission spectra of a quartz EDL at the 30 and 300 W output power (Synthewave 402).

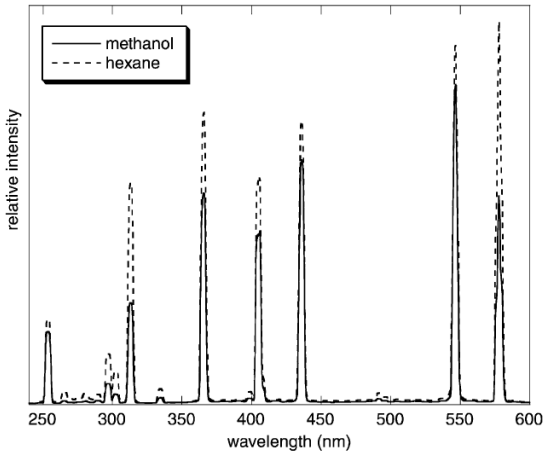

Fig. 7. Comparison of the emission spectra of a quartz EDL in *n*-hexane and methanol.

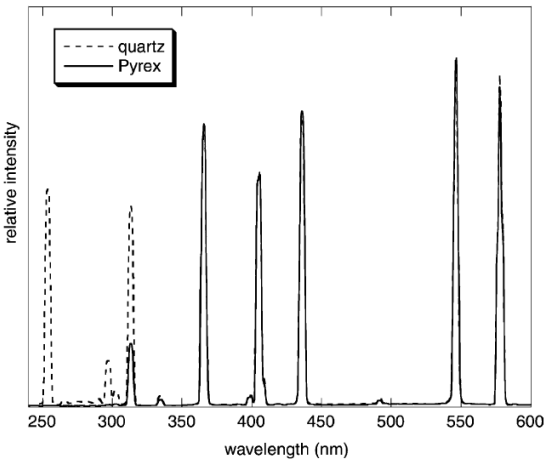

Fig. 8. A comparison of the emission spectra of quartz and Pyrex EDLs in *n*-hexane.

well explains the efficiency loss observed in photochemical experiments. The solvent can be also used as an internal UV filter. Benzene, for example, significantly suppressed the wavelengths below 280 nm (Fig. 9). Therefore, *n*-hexane or other non-polar solvents, that are transparent over 220 nm, are ideal in case a short-wavelength irradiation is required.

In conclusion, the aim of this paper was to show that the spectrum of the electrodeless discharge lamps can be easily modified by choosing a proper temperature, the EDL envelope glass material, or a solvent used in a photochemical reaction. In addition, the EDL emission intensity could be adjusted by changing the MW output power. Since the application of EDLs in photochemistry is very simple and accessible to a broad spectrum of chemists, it could find its way into a conventional chemical laboratory. Studies of EDLs that contain other filling materials than mercury are currently under investigation.

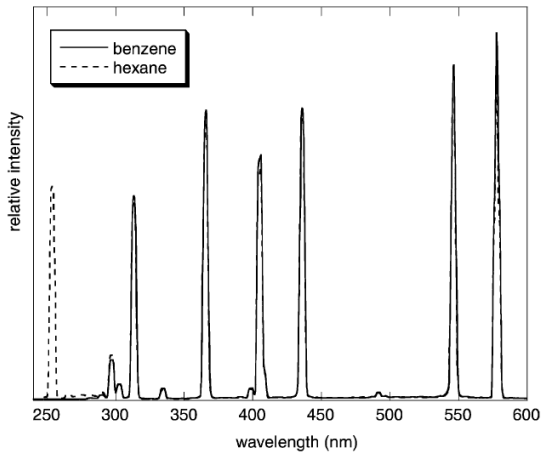

Fig. 9. A comparison of the emission spectra of a quartz EDL in *n*-hexane and benzene.

Acknowledgements

This work was supported by the Grant Agency of the Czech Republic (203/02/0879). We thank P. Janderka for an opportunity to measure the spectra on an AVS-S2000 spectrometer. We would also like to thank Z. Bohacek and the Czech Geological Survey for the purification and supply of hydrocarbons.

References

[1] Š. Toma, A. Gáplovský, J.L. Luche, Ultrason. Sonochem. 8 (2001) 201.
[2] A. Gáplovský, J. Donovalová, Š. Toma, R. Kubinec, Ultrason. Sonochem. 4 (1997) 109.
[3] A. Gáplovský, J. Donovalová, Š. Toma, R. Kubinec, J. Photochem. Photobiol. A Chem. 115 (1998) 13.
[4] H. Hayashi, Y. Sakaguchi, M. Wakasa, Bull. Chem. Soc. Jpn. 74 (2001) 773.
[5] J.R. Woodward, Prog. React. Kinet. Mech. 27 (2002) 165.
[6] P. Klán, V. Církva, Microwave photochemistry, in: A. Loupy (Ed.), Microwaves in Organic Synthesis, Wiley–VCH, Weinheim, 2002.
[7] R.A. Abramovitch, Org. Prep. Proced. Int. 23 (1991) 685.
[8] D.M.P. Mingos, D.R. Baghurst, Chem. Soc. Rev. 20 (1991) 1.
[9] A.G. Whittaker, D.M.P. Mingos, J. Microw. Power Electromagn. Energy 29 (1994) 195.
[10] S.A. Galema, Chem. Soc. Rev. 26 (1997) 233.
[11] P. Klán, J. Literák, M. Hájek, J. Photochem. Photobiol. A Chem. 128 (1999) 145.
[12] J. Literák, P. Klán, J. Photochem. Photobiol. A Chem. 137 (2000) 29.
[13] P. Klán, M. Hájek, V. Církva, J. Photochem. Photobiol. A Chem. 140 (2001) 185.
[14] I.E. Den Besten, J.W. Tracy, J. Chem. Educ. 50 (1973) 303.
[15] V. Církva, M. Hájek, J. Photochem. Photobiol. A Chem. 123 (1999) 21.
[16] J. Literák, P. Klán, D. Heger, A. Loupy, J. Photochem. Photobiol. A Chem. 154 (2002) 155.
[17] P. Klán, J. Literák, S. Relich, J. Photochem. Photobiol. A Chem. 143 (2001) 49.
[18] P. Klán, R. Ruzicka, D. Heger, J. Literák, P. Kulhánek, A. Loupy, Photochem. Photobiol. Sci. 1 (2002) 1012.
[19] A.G. Howard, L. Labonne, E. Rousay, Analyst 126 (2001) 141.
[20] D. Florian, G. Knapp, Anal. Chem. 73 (2001) 1515.
[21] S. Horikoshi, H. Hidaka, N. Serpone, J. Photochem. Photobiol. A Chem. 153 (2002) 185.
[22] S. Horikoshi, H. Hidaka, N. Serpone, Environ. Sci. Technol. 36 (2002) 5229.
[23] S.C. Brown, Introduction to Electrical Discharges in Gases, Wiley, New York, 1966.
[24] P. Spietz, U. Gross, E. Smalins, J. Orphal, J.P. Burrows, Spectrochim. Acta Part B At. Spectrom. 56 (2001) 2465.
[25] R.F. Browner, J.D. Winefordner, Spectrochim. Acta 28B (1973) 263.
[26] J. Sneddon, R.F. Browner, P.N. Keliher, J.D. Winefordner, D.J. Butcher, R.G. Michel, Prog. Anal. Spectrosc. 12 (1989) 369.
[27] N. Imamura, J. Sakaguchi, S. Asatani, S. Hashiguchi, K. Obara, J. Cryst. Growth 237 (2002) 76.
[28] J.P.S. Haarsma, G.J. DeJong, J. Agterdenbos, Spectrochim. Acta 29B (1974) 1.
[29] W.S. Gleason, R. Pertel, Rev. Sci. Instrum. 42 (1971) 1638.